PHYSICAL REVIEW D **78,** 076002 (2008)

Rescattering effects in charmless $\bar{B}_{u,d,s} \to PP$ decays

Chun-Khiang Chua

Physics Department, Chung Yuan Christian University, Chung-Li, Taiwan 32023, Republic of China

(Received 10 January 2008; published 8 October 2008)

We study the final-state interaction (FSI) effects in charmless $\bar{B}_{u,d,s} \to PP$ decays. We consider a FSI approach with both short- and long-distance contributions, where the former are from inelastic channels and are contained in factorization amplitudes, while the latter are from the residual rescattering among PP states. Flavor SU(3) symmetry is used to constrain the residual rescattering S matrix. We fit to all available data on the CP-averaged decay rates and CP asymmetries, and make predictions on unmeasured ones. We investigate the $K\pi$ direct CP violations that lead to the so-called $K\pi$ puzzle in CP violation. Our main results are as follows: (i) Results are in agreement with data in the presence of FSI. (ii) For $\bar{B}$ decays, the $\pi^+\pi^-$ and $\pi^0\pi^0$ rates are suppressed and enhanced, respectively, by FSI. (iii) The FSI has a large impact on direct CP asymmetries ($\mathcal{A}$) of many modes. (iv) The deviation ($\Delta\mathcal{A}$) between $\mathcal{A}(\bar{B}^0 \to K^-\pi^+)$ and $\mathcal{A}(B^- \to K^-\pi^0)$ can be understood in the FSI approach. Since $\mathcal{A}(K^-\pi^0)$ is more sensitive to the residual rescattering, the degeneracy of these two direct CP violations can be successfully lifted. (v) Sizable and complex color-suppressed tree amplitudes, which are crucial for the large $\pi^0\pi^0$ rate and $\Delta\mathcal{A}$, are generated through exchange rescattering. The correlation of the ratio $\mathcal{B}(\pi^0\pi^0)/\mathcal{B}(\pi^+\pi^-)$ and $\Delta\mathcal{A}$ is studied. (vi) The $B^- \to \pi^-\pi^0$ direct CP violation is very small and is not affected by FSI. (vii) Several $\bar{B}_s$ decay rates are enhanced. In particular, the $\eta'\eta'$ branching ratio is enhanced to the level of 1.0×10^{-4}, which can be checked experimentally. (viii) Time-dependent CP asymmetries S in $\bar{B}_{d,s}$ decays are studied. The $\Delta S(\bar{B}^0 \to K_S\eta')$ is very small ($\leq 1\%$). This asymmetry remains to be one of the cleanest measurements to search for new physics phases. The asymmetry S from $\bar{B}_s$ to PP states with strangeness $S = +1$ are expected to be small. We found that the $|S|$ for $\bar{B}_s^0 \to \eta\eta$, $\eta\eta'$, and $\eta'\eta'$ decays are all below 0.06. CP asymmetries in these modes will be useful to test the SM.

DOI: 10.1103/PhysRevD.78.076002 PACS numbers: 11.30.Hv, 13.25.Hw, 14.40.Nd

I. INTRODUCTION

The study of B decays provides many useful information of the flavor sector of the standard model (SM) [1]. In particular, the measurements of the time-dependent CP asymmetries in kaon and charmonium final states give a rather precise value of $\sin 2\beta = 0.681 \pm 0.025$ [2], where $\beta/\phi_1 = \arg(V_{td}^*)$ with V the Cabbibo-Kobayashi-Mashikawa (CKM) matrix. In the SM, time-dependent CP asymmetries in penguin dominated modes are expected to be close to the $\sin 2\beta$ value [3]. Since the penguin loop amplitudes are sensitive to high virtuality, new physics beyond the SM may contribute to the time-dependent CP asymmetries through the heavy particles in the loops. Consequently, these asymmetries are promising places to search for new physics effects [3–8].

The measurements of direct CP violation ($\mathcal{A}$) in $\bar{B}$ decays are also very useful and interesting. The $\mathcal{A}(\bar{B}^0 \to K^-\pi^+)$ asymmetry was the first measured direct CP violation in $\bar{B}$ decays. The data confirmed a large $\mathcal{A}(\bar{B}^0 \to K^-\pi^+)$ with a negative sign as predicted in perturbative QCD calculations [9]. On the contrary, although $\mathcal{A}(B^- \to K^-\pi^0) \simeq \mathcal{A}(\bar{B}^0 \to K^-\pi^+)$ was expected in many early theoretical predictions [9,10], the experimental evidence has been accumulated favoring a positive $\mathcal{A}(B^- \to K^-\pi^0)$. The recent measurements show $\mathcal{A}(K^-\pi^+) = (-9.8^{+1.2}_{-1.1})\%$ and $\mathcal{A}(K^-\pi^0) = (5.0 \pm 2.5)\%$ [2], giving $\Delta\mathcal{A}(K\pi) \equiv \mathcal{A}(K^-\pi^0) - \mathcal{A}(K^-\pi^+) = (14.8^{+2.7}_{-2.8})\%$, which is more than 5σ from zero. This is the so-called $K\pi$ puzzle in direct CP violation, which has attracted a lot of attention [11–19]. Several suggestions were put forth to resolve this puzzle. For example, some authors introduced next-to-leading order contributions in factorization amplitudes [14], while some suggested new physics origins [11–13,16–19] for the deviation.

It is well known that we need both weak and strong phase differences to have a nonvanishing direct CP violation. Strictly speaking, the final-state interaction (FSI) is the only source for nonvanishing strong phases. In addition, it is capable of enhancing the decay rates of many modes, which are measured to be larger than expected. For example, the large observed $\bar{B}^0 \to \pi^0\pi^0$ rate, which remains puzzling and is still posing tension in many theoretical calculations, can be obtained by using FSI [20]. Furthermore, it was recently realized that long-distance FSI may play an indispensable role in charmful as well as in charmless $\bar{B}$ decays [21,22].

Data for $\bar{B}_s$ decays are starting to emerge from the Tevetron [1] and from B factories, and we anticipate more to come in the near future, from LHCb and other LHC experiments. Measurements of rates and CP asymmetries in $\bar{B}_s$ decays will be useful in testing the SM and in searching for new (physics) phases. In fact, recently, a claim on the evidence of new physics effect in the $\bar{B}_s$

mixing was put forth [23]. It is thus timely to study $\bar{B}_s$ decays.

In this work, we investigate the effects of FSI on all charmless $\bar{B}_{u,d,s} \to PP$ decay rates and CP asymmetries. We outline the underlying physical picture of the FSI approach employed in this work. The master formula of FSI for charmless $\bar{B} \to PP$ decays is (see appendix A, if a derivation is needed)

$$A_i^{\rm FSI} = \sum_{k=1}^{N} \mathcal{S}_{ik}^{1/2} A_k^0, \tag{1}$$

where $A^{\rm FSI}$ and A^0 are $\bar{B}$ decay amplitudes with and without FSI,[1] respectively, $i = 1, \ldots, n$ denotes all charmless PP states, $k = 1, \ldots, n, n+1, \ldots, N$ denotes *all* possible states that can rescatter into the charmless PP states, and $\mathcal{S}$ is the strong interacting S matrix. Note that no approximation has been made in the above equation, which, in principle, all charmless $\bar{B}$ decay amplitudes should follow. In practice, this master formula is hard to use as it involves many states (the number N is in general quite large in a typical charmless B decay).

Let us investigate further the difficulties of using the above master formula. The number of states allowed to enter the formula grows with the mass of the decaying particle. For a typical B decay, there is a large number of the states involved in the equation and the contributions are hard to handle. For example, we may need to consider a rescattering process contributed from a multibody final state, where the decay amplitude and the corresponding rescattering S-matrix element are poorly known. Therefore, the complication originates from the largeness of m_B. However, it is precisely the largeness of m_B that makes factorization approaches such as perturbative QCD [9], QCD factorization (QCDF) [10,24] and soft collinear effective theory [25] possible. These approaches achieve accessibility and simplifications. The underlying reason for the simplicity is related to the so-called duality argument, which uses the fact that when contributions from all hadronic states at a large enough energy scale are summed over, one should be able to understand the physics in terms of the quark and gluon degrees of freedom. Hence, it is reasonable to expect that the main effect of FSI, especially those from inelastic channels, is included in the factorization amplitudes—a statement we expect to hold perfectly in the $m_b \to \infty$ case. Since in the real world m_b is finite, whether it is large enough to validate the above argument should be answered by experiments.

It is fair to say that most factorization results on CP-averaged charmless $\bar{B} \to PP$ decay rates, especially color-allowed ones, agree well with the data. However, some measurements seem to imply the needs of subleading contributions. For example, rates of some suppressed decay modes, such as the above mentioned $\bar{B}^0 \to \pi^0\pi^0$ rate, and some CP-odd quantities, such as the $B^- \to K^-\pi^0$ direct CP violation, do not agree well with predictions. These are places, where subleading effects, such as FSI, could be visible. Therefore, although we expect factorization amplitudes to contain most of the FSI effects demanded in Eq. (1), it is likely that residual rescattering is still allowed and needed in $\bar{B} \to PP$ decays at the physical m_B energy scale. The group of charmless PP states is unique to the processes we are studying and is well separated from all other states. Since the duality argument cannot be applied to these states of limited number, part of their FSI effects may not be included in the factorization amplitudes [26,27].

In summary, FSI in B decays may be simpler than we thought, since m_B could be large enough to apply a factorization approach for the main part of FSI contributions. We may only need to include the leftover FSI, i.e. residual rescattering, in addition to the short-distance FSI in the PP sector. In this sense, the FSI approach we are using is a mild extension to the factorization approaches.

Note that a similar approach analyzing early data was used in [27]. There is one major difference. In [27], in principle, no short-distance phase was allowed in factorization amplitudes to avoid double counting, while here we do need short-distance phases to account for the FSI effects from all inelastic plus some quasi-elastic channels. There are also other works in the literature discussing rescattering among PP states and/or from some inelastic channels [22,28–32]. For example, in [22], rescattering from PP and $D^{(*)}\bar{D}^{(*)}$ final states was considered, and the main FSI contributions resemble the charming penguin ones [32,33]. We also note that similar discussion of the factorization of $\mathcal{S}$ into short-distance and residual parts, as well as the discussion of the approximation done when assuming S is block diagonal (with a block for the PP states) can be found in [28].

The layout of the present paper is as follows: In Sec. II, we introduce the formalism. We then use it in Sec. III to study $\bar{B}_{u,d,s} \to PP$ decays. Results and discussions are also presented. Section IV contains our conclusions. Some derivations, including those lead to Eq. (1), are given in appendices.

II. FORMALISM

In this section, we develop the formalism. The reader who is not interested in the detail of the formalism may proceed directly to the numerical analysis section.

Without loss of generality, we can re-express the S matrix in Eq. (1) as

$$\mathcal{S}_{ik} = \sum_{j=1}^{n} (\mathcal{S}_1)_{ij} (\mathcal{S}_2)_{jk}, \tag{2}$$

where $\mathcal{S}_1$ is a nonsingular $n \times n$ matrix with n as the total

[1]Note that $A^{\rm FSI}$ contains weak as well as strong phases, while A^0 only has weak phases.

number of charmless PP states and $\mathcal{S}_2$ is defined through the above equation, i.e. $\mathcal{S}_2 \equiv \mathcal{S}_1^{-1}\mathcal{S}$. The physical picture mentioned in the last section is close to the one in factorization approaches, except that there are still some residual rescattering effects, and we have

$$\mathcal{S}_1 = \mathcal{S}_{\rm res}, \qquad A_j^{\rm fac} = \sum_{k=1}^{N} (\mathcal{S}_2^{1/2})_{jk} A_k^0, \tag{3}$$

with N as the total number of states entering Eq. (1) and $A_j^{\rm fac}$ as the factorization amplitude. The residual rescattering effect is encoded in the $\mathcal{S}_{\rm res}$ matrix. Note that although $\mathcal{S}$ is unitary, $\mathcal{S}_{\rm res}$ needs not be so, as it describes the residual rescattering among various charmless PP states. In factorization approaches, the above $\mathcal{S}_{\rm res}$ is taken to be unity. We shall use the up-to-date data to determine $\mathcal{S}_{\rm res}$. It should be reminded that our framework does not exclude the fully factorized case ($\mathcal{S}_{\rm res} = 1$) and, hence, it is also being tested. To apply the above formula, we need to specify the factorization amplitudes. In this work, we use the factorization amplitudes obtained in the QCD factorization approach [24].

Combining Eqs. (1) and (3), we have

$$A_i^{\rm FSI} = \sum_{j=1}^{n} (\mathcal{S}_{\rm res}^{1/2})_{ij} A_j^{\rm fac}, \tag{4}$$

where, as mentioned before, $i,\ j = 1, \ldots, n$ denote all charmless PP states. The number of parameters needed to describe $\mathcal{S}_{\rm res}$ seems to be quite large. This is, however, not the case, since strong interaction has (an approximate) SU(3) symmetry, which is expected to be a good one at the m_B rescattering scale and, hence, can be used to constrain the form of $S_{\rm res}$.

Explicitly, through SU(3) symmetry, we have

$$\begin{pmatrix} A^{\rm FSI}_{\bar B^0_{d,s}\to K^-\pi^+} \\ A^{\rm FSI}_{\bar B^0_{d,s}\to \bar K^0\pi^0} \\ A^{\rm FSI}_{\bar B^0_{d,s}\to \bar K^0\eta_8} \\ A^{\rm FSI}_{\bar B^0_{d,s}\to \bar K^0\eta_1} \end{pmatrix} = \mathcal{S}_{{\rm res},1}^{1/2} \begin{pmatrix} A^{\rm fac}_{\bar B^0_{d,s}\to K^-\pi^+} \\ A^{\rm fac}_{\bar B^0_{d,s}\to \bar K^0\pi^0} \\ A^{\rm fac}_{\bar B^0_{d,s}\to \bar K^0\eta_8} \\ A^{\rm fac}_{\bar B^0_{d,s}\to \bar K^0\eta_1} \end{pmatrix}, \tag{5}$$

$$\begin{pmatrix} A^{\rm FSI}_{B^-\to \bar K^0\pi^-} \\ A^{\rm FSI}_{B^-\to K^-\pi^0} \\ A^{\rm FSI}_{B^-\to K^-\eta_8} \\ A^{\rm FSI}_{B^-\to K^-\eta_1} \end{pmatrix} = \mathcal{S}_{{\rm res},2}^{1/2} \begin{pmatrix} A^{\rm fac}_{B^-\to \bar K^0\pi^-} \\ A^{\rm fac}_{B^-\to K^-\pi^0} \\ A^{\rm fac}_{B^-\to K^-\eta_8} \\ A^{\rm fac}_{B^-\to K^-\eta_1} \end{pmatrix}, \tag{6}$$

$$\begin{pmatrix} A^{\rm FSI}_{B^-\to \pi^-\pi^0} \\ A^{\rm FSI}_{B^-\to K^0K^-} \\ A^{\rm FSI}_{B^-\to \pi^-\eta_8} \\ A^{\rm FSI}_{B^-\to \pi^-\eta_1} \end{pmatrix} = \mathcal{S}_{{\rm res},3}^{1/2} \begin{pmatrix} A^{\rm fac}_{B^-\to \pi^-\pi^0} \\ A^{\rm fac}_{B^-\to K^0K^-} \\ A^{\rm fac}_{B^-\to \pi^-\eta_8} \\ A^{\rm fac}_{B^-\to \pi^-\eta_1} \end{pmatrix}, \tag{7}$$

$$\begin{pmatrix} A^{\rm FSI}_{\bar B^0_{d,s}\to \pi^+\pi^-} \\ A^{\rm FSI}_{\bar B^0_{d,s}\to \pi^0\pi^0} \\ A^{\rm FSI}_{\bar B^0_{d,s}\to \eta_8\eta_8} \\ A^{\rm FSI}_{\bar B^0_{d,s}\to \eta_8\eta_1} \\ A^{\rm FSI}_{\bar B^0_{d,s}\to \eta_1\eta_1} \\ A^{\rm FSI}_{\bar B^0_{d,s}\to K^+K^-} \\ A^{\rm FSI}_{\bar B^0_{d,s}\to K^0\bar K^0} \\ A^{\rm FSI}_{\bar B^0_{d,s}\to \pi^0\eta_8} \\ A^{\rm FSI}_{\bar B^0_{d,s}\to \pi^0\eta_1} \end{pmatrix} = \mathcal{S}_{{\rm res},4}^{1/2} \begin{pmatrix} A^{\rm fac}_{\bar B^0_{d,s}\to \pi^+\pi^-} \\ A^{\rm fac}_{\bar B^0_{d,s}\to \pi^0\pi^0} \\ A^{\rm fac}_{\bar B^0_{d,s}\to \eta_8\eta_8} \\ A^{\rm fac}_{\bar B^0_{d,s}\to \eta_8\eta_1} \\ A^{\rm fac}_{\bar B^0_{d,s}\to \eta_1\eta_1} \\ A^{\rm fac}_{\bar B^0_{d,s}\to K^+K^-} \\ A^{\rm fac}_{\bar B^0_{d,s}\to K^0\bar K^0} \\ A^{\rm fac}_{\bar B^0_{d,s}\to \pi^0\eta_8} \\ A^{\rm fac}_{\bar B^0_{d,s}\to \pi^0\eta_1} \end{pmatrix}, \tag{8}$$

where we have $\mathcal{S}_{{\rm res},i}^{1/2} = (1 + i\mathcal{T}_i)^{1/2}$, with

$$\mathcal{T}_1 = \begin{pmatrix} r_0 + r_a & \frac{-r_a+r_e}{\sqrt{2}} & \frac{-r_a+r_e}{\sqrt{6}} & \frac{2\bar r_a+\bar r_e}{\sqrt{3}} \\ \frac{-r_a+r_e}{\sqrt{2}} & r_0 + \frac{r_a+r_e}{2} & \frac{r_a-r_e}{2\sqrt{3}} & -\frac{2\bar r_a+\bar r_e}{3\sqrt{2}} \\ \frac{-r_a+r_e}{\sqrt{6}} & \frac{r_a-r_e}{2\sqrt{3}} & r_0 + \frac{r_a+5r_e}{6} & -\frac{2\bar r_a+\bar r_e}{3\sqrt{2}} \\ \frac{2\bar r_a+\bar r_e}{\sqrt{3}} & -\frac{2\bar r_a+\bar r_e}{\sqrt{6}} & -\frac{2\bar r_a+\bar r_e}{3\sqrt{2}} & \tilde r_0 + \frac{4\bar r_a+2\bar r_e}{3} \end{pmatrix},$$

$$\mathcal{T}_2 = \begin{pmatrix} r_0 + r_a & \frac{r_a-r_e}{\sqrt{2}} & \frac{-r_a+r_e}{\sqrt{6}} & \frac{2\bar r_a+\bar r_e}{\sqrt{3}} \\ \frac{r_a-r_e}{\sqrt{2}} & r_0 + \frac{r_a+r_e}{2} & \frac{-r_a+r_e}{2\sqrt{3}} & \frac{2\bar r_a+\bar r_e}{3\sqrt{2}} \\ \frac{-r_a+r_e}{\sqrt{6}} & \frac{-r_a+r_e}{2\sqrt{3}} & r_0 + \frac{r_a+5r_e}{6} & -\frac{2\bar r_a+\bar r_e}{3\sqrt{2}} \\ \frac{2\bar r_a+\bar r_e}{\sqrt{3}} & \frac{2\bar r_a+\bar r_e}{\sqrt{6}} & -\frac{2\bar r_a+\bar r_e}{3\sqrt{2}} & \tilde r_0 + \frac{4\bar r_a+2\bar r_e}{3} \end{pmatrix}, \tag{9}$$

$$\mathcal{T}_3 = \begin{pmatrix} r_0 + r_a & 0 & 0 & 0 \\ 0 & r_0 + r_a & \sqrt{\frac{2}{3}}(r_a - r_e) & \frac{2\bar r_a+\bar r_e}{\sqrt{3}} \\ 0 & \sqrt{\frac{2}{3}}(r_a - r_e) & r_0 + \frac{2r_a+r_e}{3} & \frac{\sqrt{2}}{3}(2\bar r_a + \bar r_e) \\ 0 & \frac{2\bar r_a+\bar r_e}{\sqrt{3}} & \frac{\sqrt{2}}{3}(2\bar r_a + \bar r_e) & \tilde r_0 + \frac{4\bar r_a+2\bar r_e}{3} \end{pmatrix},$$

and

$$\mathcal{T}_4 = \mathrm{diag}(r_0, r_0, r_0, \tilde{r}_0, \check{r}_0, r_0, r_0, r_0, \tilde{r}_0)$$

$$+\begin{pmatrix}
2r_a + r_t & \frac{2r_a - r_e + r_t}{\sqrt{2}} & \frac{2r_a + r_e + 3r_t}{3\sqrt{2}} & \frac{\sqrt{2}(2\bar{r}_a + \bar{r}_e)}{3} & \frac{4\hat{r}_a + 2\hat{r}_e + 3\hat{r}_t}{3\sqrt{2}} & r_a + r_t & r_a + r_t & 0 & 0 \\
\frac{2r_a - r_e + r_t}{\sqrt{2}} & \frac{2r_a + r_e + r_t}{2} & \frac{2r_a + r_e + 3r_t}{6} & \frac{2\bar{r}_a + \bar{r}_e}{3} & \frac{4\hat{r}_a + 2\hat{r}_e + 3\hat{r}_t}{6} & \frac{r_a + r_t}{\sqrt{2}} & \frac{r_a + r_t}{\sqrt{2}} & 0 & 0 \\
\frac{2r_a + r_e + 3r_t}{3\sqrt{2}} & \frac{2r_a + r_e + 3r_t}{6} & \frac{2r_a + r_e + r_t}{2} & -\frac{2\bar{r}_a + \bar{r}_e}{3} & \frac{4\hat{r}_a + 2\hat{r}_e + 3\hat{r}_t}{6} & \frac{5r_a - 2r_e + 3r_t}{3\sqrt{2}} & \frac{5r_a - 2r_e + 3r_t}{3\sqrt{2}} & 0 & 0 \\
\frac{\sqrt{2}(2\bar{r}_a + \bar{r}_e)}{3} & \frac{2\bar{r}_a + \bar{r}_e}{3} & -\frac{2\bar{r}_a + \bar{r}_e}{3} & \frac{4\tilde{r}_a + 2\tilde{r}_e}{3} & 0 & -\frac{2\bar{r}_a + \bar{r}_e}{3\sqrt{2}} & -\frac{2\bar{r}_a + \bar{r}_e}{3\sqrt{2}} & 0 & 0 \\
\frac{4\hat{r}_a + 2\hat{r}_e + 3\hat{r}_t}{3\sqrt{2}} & \frac{4\hat{r}_a + 2\hat{r}_e + 3\hat{r}_t}{6} & \frac{4\hat{r}_a + 2\hat{r}_e + 3\hat{r}_t}{6} & 0 & \frac{4\check{r}_a + 2\check{r}_e + 3\check{r}_t}{6} & \frac{4\hat{r}_a + 2\hat{r}_e + 3\hat{r}_t}{3\sqrt{2}} & \frac{4\hat{r}_a + 2\hat{r}_e + 3\hat{r}_t}{3\sqrt{2}} & 0 & 0 \\
r_a + r_t & \frac{r_a + r_t}{\sqrt{2}} & \frac{5r_a - 2r_e + 3r_t}{3\sqrt{2}} & -\frac{2\bar{r}_a + \bar{r}_e}{3\sqrt{2}} & \frac{4\hat{r}_a + 2\hat{r}_e + 3\hat{r}_t}{3\sqrt{2}} & 2r_a + r_t & r_a + r_t & \frac{r_a - r_e}{\sqrt{3}} & \frac{2\bar{r}_a + \bar{r}_e}{\sqrt{6}} \\
r_a + r_t & \frac{r_a + r_t}{\sqrt{2}} & \frac{5r_a - 2r_e + 3r_t}{3\sqrt{2}} & -\frac{2\bar{r}_a + \bar{r}_e}{3\sqrt{2}} & \frac{4\hat{r}_a + 2\hat{r}_e + 3\hat{r}_t}{3\sqrt{2}} & r_a + r_t & 2r_a + r_t & \frac{-r_a + r_e}{\sqrt{3}} & -\frac{2\bar{r}_a + \bar{r}_e}{\sqrt{6}} \\
0 & 0 & 0 & 0 & 0 & \frac{r_a - r_e}{\sqrt{3}} & \frac{-r_a + r_e}{\sqrt{3}} & \frac{2r_a + r_e}{3} & \frac{\sqrt{2}(2\bar{r}_a + \bar{r}_e)}{3} \\
0 & 0 & 0 & 0 & 0 & \frac{2\bar{r}_a + \bar{r}_e}{\sqrt{6}} & -\frac{2\bar{r}_a + \bar{r}_e}{\sqrt{6}} & \frac{\sqrt{2}(2\bar{r}_a + \bar{r}_e)}{3} & \frac{4\tilde{r}_a + 2\tilde{r}_e}{3}
\end{pmatrix}. \tag{10}$$

The rescattering parameters $r_{0,a,e,t}$, $\bar{r}_{0,a,e,t}$, $\tilde{r}_{0,a,e,t}$, $\hat{r}_{0,a,e,t}$, and $\check{r}_{0,a,e,t}$ denote rescattering in $\Pi(\mathbf{8})\Pi(\mathbf{8}) \to \Pi(\mathbf{8})\Pi(\mathbf{8})$, $\Pi(\mathbf{8})\Pi(\mathbf{8}) \to \Pi(\mathbf{8})\eta_1$, $\Pi(\mathbf{8})\eta_1 \to \Pi(\mathbf{8})\eta_1$, and $\eta_1\eta_1 \to \eta_1\eta_1$, respectively, and the subscripts 0, a, e, t represent flavor singlet, annihilation, exchange, and total-annihilation rescatterings, respectively, (see Fig. 1). Note that for identical particle final states, such as $\pi^0\pi^0$, factors of $1/\sqrt{2}$ are included in the amplitudes and the corresponding $\mathcal{S}_{\rm res}$ matrix elements. The $P\eta_8$, $P\eta_1$ are not physical final states. The physical η, η' mesons are defined through

$$\begin{pmatrix} \eta \\ \eta' \end{pmatrix} = \begin{pmatrix} \cos\vartheta & -\sin\vartheta \\ \sin\vartheta & \cos\vartheta \end{pmatrix} \begin{pmatrix} \eta_8 \\ \eta_1 \end{pmatrix}, \tag{11}$$

with the mixing angle $\vartheta \simeq -15.4°$ [34]. For the $\eta^{(\prime)}\eta^{(\prime)}$ states, we have

$$\begin{pmatrix} \eta\eta \\ \eta\eta' \\ \eta'\eta' \end{pmatrix} = \begin{pmatrix} \cos^2\vartheta & -\sqrt{2}\cos\vartheta\sin\vartheta & \sin^2\vartheta \\ \sqrt{2}\cos\vartheta\sin\vartheta & \cos^2\vartheta - \sin^2\vartheta & -\sqrt{2}\cos\vartheta\sin\vartheta \\ \sin^2\vartheta & \sqrt{2}\cos\vartheta\sin\vartheta & \cos^2\vartheta \end{pmatrix} \begin{pmatrix} \eta_8\eta_8 \\ \eta_8\eta_1 \\ \eta_1\eta_1 \end{pmatrix}, \tag{12}$$

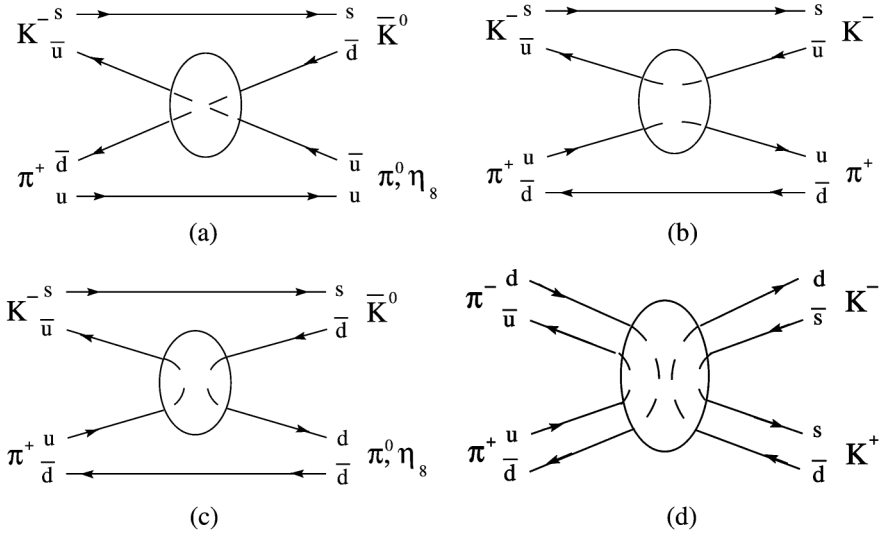

FIG. 1. Pictorial representation of (a) charge exchange r_e, (b) singlet exchange r_0, (c) annihilation r_a and (d) total-annihilation r_t for PP (re)scattering.

where the identical particle factor of $1/\sqrt{2}$ is properly included in the mixing matrix.

The matrices $\mathcal{T}_{1,2,3,4}$ can be obtained through a diagrammatic method by matching the Clebsh-Gordan coefficients of scattering mesons (see Fig. 1) or by using an operator method. We have $\mathrm{Tr}(\Pi_1^{\mathrm{in}}\Pi_1^{\mathrm{out}}\Pi_2^{\mathrm{in}}\Pi_2^{\mathrm{out}})/2$, $\mathrm{Tr}(\Pi_1^{\mathrm{in}}\Pi_2^{\mathrm{in}}\Pi_1^{\mathrm{out}}\Pi_2^{\mathrm{out}})$, $\mathrm{Tr}(\Pi_1^{\mathrm{in}}\Pi_1^{\mathrm{out}})\mathrm{Tr}(\Pi_2^{\mathrm{in}}\Pi_2^{\mathrm{out}})$, and $\mathrm{Tr}(\Pi_1^{\mathrm{in}}\Pi_2^{\mathrm{in}})\mathrm{Tr}(\Pi_1^{\mathrm{out}}\Pi_2^{\mathrm{out}})$ corresponding to r_e, r_a, r_0, and r_t contributions, respectively, (see similar discussion for the case of charmful B decays in [21]). Note that due to Bose-Einstein statistic and the S-wave configuration of the final-state mesons in $\bar{B} \to P_1P_2$ decays, the amplitude should be symmetric under the exchange of the indices 1 and 2. Consequently, the above terms exhaust all possible combinations for $\Pi(\mathbf{8})\Pi(\mathbf{8}) \to \Pi(\mathbf{8})\Pi(\mathbf{8})$ scatterings. For operators involving η_1, we suitably replace Π in the above expressions by $\eta_1 1_{3\times3}$ to obtain operators corresponding to $\bar{r}_i$, $\tilde{r}_i$, $\hat{r}_i$, and $\check{r}_i$.

It can be easily seen that rescattering formulas for charmless $\bar{B}_s \to PP$ decays resemble those for $\bar{B}^0 \to PP$ decays. Information on $\mathcal{S}_{\mathrm{rec}}$ obtained from $\bar{B}_d^0$ decays can be used to predict $\bar{B}_s$ decay rates.

At first sight, it appears that we need 40 real parameters (from 20 complex rescattering parameters: $r_{0,a,e,t}$, $\bar{r}_{0,a,e,t}$, $\tilde{r}_{0,a,e,t}$, $\hat{r}_{0,a,e,t}$, and $\check{r}_{0,a,e,t}$) to describe $\mathcal{S}_{\mathrm{res}}$. The number of independent parameters is actually much lower for two reasons. First, rescattering parameters enter $\mathcal{S}_{\mathrm{res}}$ only through 7 independent combinations: $1 + i(r_0 + r_a)$, $i(r_e - r_a)$, $i(r_a + r_t)$, $i(2\bar{r}_a + \bar{r}_e)$, $1 + i[\tilde{r}_0 + (4\tilde{r}_a + 2\tilde{r}_e)/3]$, $i(4\hat{r}_a + 2\hat{r}_e + 3\hat{r}_t)$, and $1 + i[\check{r}_0 + (4\check{r}_a + 2\check{r}_e + 3\check{r}_t)/6]$. Second, SU(3) symmetry imposes further constraints on these combinations.

Flavor symmetry requires that $(\mathcal{S}_{\mathrm{res}})^m$ with an arbitrary power of m should also have the same form as $\mathcal{S}_{\mathrm{res}}$. More explicitly, from SU(3) symmetry, we should have

$$(\mathcal{S}_{\mathrm{res}})^m = (1 + i\mathcal{T})^m \equiv 1 + i\mathcal{T}^{(m)}, \tag{13}$$

where $\mathcal{T}^{(m)}$ is defined through the above equation and its form is given by

$$\mathcal{T}^{(m)} = \mathcal{T} \quad \text{with } (r_j, \bar{r}_j, \tilde{r}_j, \check{r}_j) \to (r_j^{(m)}, \bar{r}_j^{(m)}, \tilde{r}_j^{(m)}, \check{r}_j^{(m)}), \tag{14}$$

for $j = 0, a, e, t$.

It is found that the solutions to Eqs. (13) and (14) are given by

$$1 + i(r_0^{(m)} + r_a^{(m)}) = \frac{2e^{2mi\delta_{27}} + 3\mathcal{U}_{11}^m}{5}, \qquad i(r_e^{(m)} - r_a^{(m)}) = \frac{3e^{2mi\delta_{27}} - 3\mathcal{U}_{11}^m}{5},$$
$$i(r_a^{(m)} + r_t^{(m)}) = \frac{-e^{2mi\delta_{27}} - 4\mathcal{U}_{11}^m + 5\mathcal{V}_{11}^m}{20}, \qquad i(2\bar{r}_a^{(m)} + \bar{r}_e^{(m)}) = \frac{3}{\sqrt{5}}\mathcal{U}_{12}^m, \qquad 1 + i\left(\tilde{r}_0^{(m)} + \frac{4\tilde{r}_a^{(m)} + 2\tilde{r}_e^{(m)}}{3}\right) = \mathcal{U}_{22}^m,$$
$$i(4\hat{r}_a^{(m)} + 2\hat{r}_e^{(m)} + 3\hat{r}_t^{(m)}) = \frac{3}{\sqrt{2}}\mathcal{V}_{12}^m, \qquad 1 + i\left(\check{r}_0^{(m)} + \frac{4\check{r}_a^{(m)} + 2\check{r}_e^{(m)} + 3\check{r}_t}{6}\right) = \mathcal{V}_{22}^m, \tag{15}$$

where $\mathcal{U}_{ij}^m$ and $\mathcal{V}_{ij}^m$ are elements of

$$\mathcal{U}^m(\tau, \delta_8, \delta_8') \equiv \begin{pmatrix} \cos\tau & \sin\tau \\ -\sin\tau & \cos\tau \end{pmatrix}\begin{pmatrix} e^{2mi\delta_8} & 0 \\ 0 & e^{2mi\delta_8'} \end{pmatrix}\begin{pmatrix} \cos\tau & -\sin\tau \\ \sin\tau & \cos\tau \end{pmatrix},$$
$$\mathcal{V}^m(\nu, \delta_1, \delta_1') \equiv \begin{pmatrix} \cos\nu & \sin\nu \\ -\sin\nu & \cos\nu \end{pmatrix}\begin{pmatrix} e^{2mi\delta_1} & 0 \\ 0 & e^{2mi\delta_1'} \end{pmatrix}\begin{pmatrix} \cos\nu & -\sin\nu \\ \sin\nu & \cos\nu \end{pmatrix}, \tag{16}$$

respectively. From the above solution, we see that two real mixing angles τ and ν, and five *complex* phases $\delta_{27,8,1}$, $\delta_{8,1}'$ are needed to describe $(\mathcal{S}_{\mathrm{res}})^m$ in the full SU(3) case.

Several remarks are in order. (i) The subscripts of phases denote the corresponding SU(3) multiplets and more details will be given shortly. (ii) The imaginary parts of $\delta_{27,8,1}$, $\delta_{8,1}'$ control the leakage of the nonunitary $\mathcal{S}_{\mathrm{res}}^m$ through the scattering of PP states into non-PP states. (iii) As we shall see, the $\mathcal{S}_{\mathrm{res}}^m$ can be factorized into two parts depending only on the real and the imaginary parts of these phases, respectively. (vi) To reduce the number of the FSI parameters we will consider a restricted SU(3) case, which is close to a U(3) symmetric case.

Since charmless mesons P consist of an octet ($\Pi(\mathbf{8})$) and an singlet (η_1), we have $\mathbf{8} \otimes \mathbf{8}$, $\mathbf{8} \otimes \mathbf{1}$, $\mathbf{1} \otimes \mathbf{8}$, and $\mathbf{1} \otimes \mathbf{1}$ SU(3) products for P_1P_2 final states. Because of the S-wave configuration of P_1P_2 in $\bar{B}$ decays and the Bose-Einstein statistics, the resulting SU(3) multiplets should be symmetric under the exchange of P_1 and P_2. The allowed ones are the $\mathbf{27}$, $\mathbf{8}$ and the $\mathbf{1}$ from $\mathbf{8} \otimes \mathbf{8}$, the $\mathbf{8}'$ from the symmetrized $\mathbf{8} \otimes \mathbf{1} + \mathbf{1} \otimes \mathbf{8}$, and $\mathbf{1}'$ from $\mathbf{1} \otimes \mathbf{1}$ (see, for example [35]). Hence, from SU(3) symmetry and the

Bose-Einstein statistics, we have

$$(\mathcal{S}_{\rm res})^m = \sum_{a=1}^{27} |\mathbf{27};a\rangle e^{2mi\delta_{27}}\langle \mathbf{27};a| + \sum_{b=1}^{8}\sum_{p,q=8,8'} |p;b\rangle \mathcal{U}^m_{pq}\langle q;b| + \sum_{p,q=1,1'} |p;1\rangle \mathcal{V}^m_{pq}\langle q;1|, \quad (17)$$

where a and b are labels of states within multiplets. It can be easily seen that the above form of $\mathcal{S}^m_{\rm res}$ is preserved for any value of m. We note that similar formulas for $\bar{B}\to PP$ rescattering (excluding $P=\eta_1$) from SU(3) symmetry have been used in [27,28].

From Eq. (17), we see that the matrix $\mathcal{S}^m_{\rm res}$ is in block-diagonal form and we also have

$$\begin{aligned}\mathcal{U}^m(\tau,\delta_8,\delta_8') &= \mathcal{U}^m(\tau,{\rm Re}\delta_8,{\rm Re}\delta_8')\cdot\mathcal{U}^m(\tau,i{\rm Im}\delta_8,i{\rm Im}\delta_8'),\\ \mathcal{V}^m(\nu,\delta_1,\delta_1') &= \mathcal{V}^m(\nu,{\rm Re}\delta_1,{\rm Re}\delta_1')\cdot\mathcal{V}^m(\nu,i{\rm Im}\delta_1,i{\rm Im}\delta_1'),\end{aligned} \quad (18)$$

which can be proved by using the explicit expressions of $\mathcal{U}^m$ and $\mathcal{V}^m$ given in Eq. (16). Consequently, the matrix $\mathcal{S}^m_{\rm res}$ can be factorized into two matrices containing only real and imaginary phases, respectively, i.e.

$$\mathcal{S}^m_{\rm res}(\tau,\nu;\delta_{1,8,27},\delta'_{1,8}) = \mathcal{S}^m_{\rm res}(\tau,\nu;{\rm Re}\delta_{1,8,27},{\rm Re}\delta'_{1,8})\cdot\mathcal{S}^m_{\rm res}(\tau,\nu;i{\rm Im}\delta_{1,8,27},i{\rm Im}\delta'_{1,8}). \quad (19)$$

Note that $\mathcal{S}^m_{\rm res}(\tau,\nu;i{\rm Im}\delta_i,i{\rm Im}\delta_i')$ is a $n\times n$ real matrix. Substituting the above expression of $S^{1/2}_{\rm res}$ into Eq. (4), we have

$$A_{\rm FSI} = \mathcal{S}^{1/2}_{\rm res}(\tau,\nu;{\rm Re}\delta_{1,8,27},{\rm Re}\delta'_{1,8})\cdot\mathcal{S}^{1/2}_{\rm res}(\tau,\nu;i{\rm Im}\delta_{1,8,27},i{\rm Im}\delta'_{1,8})\cdot A_{\rm fac}. \quad (20)$$

An overall phase in Eq. (20) can be removed and we are free to set ${\rm Re}\delta_{27}=0$. Furthermore, in our analysis (as well as in many analyses using naive or QCD factorization approaches), various form factors and m_s in $A_{\rm fac}$ are allowed to float in some given ranges of values. Therefore, an overall scaling factor ($\exp(-{\rm Im}\delta_{27})$) can be absorbed into the form factors in $A_{\rm fac}$ and we set ${\rm Im}\delta_{27}=0$ to avoid double counting. We are left with two mixing angles, four real phase differences, and four imaginary phase differences

$$\tau,\ \nu,\ \delta^{(\prime)}\equiv{\rm Re}(\delta_{8^{(\prime)}}-\delta_{27}),\qquad \sigma^{(\prime)}\equiv{\rm Re}(\delta_{1^{(\prime)}}-\delta_{27}),$$
$$\kappa^{(\prime)}\equiv{\rm Im}(\delta_{8^{(\prime)}}-\delta_{27}),\qquad \xi^{(\prime)}\equiv{\rm Im}(\delta_{1^{(\prime)}}-\delta_{27}). \quad (21)$$

The number of the residual FSI parameters is still quite large. It will be preferable to reduce it through some physical arguments or the consideration of some plausible cases.

It is interesting to see how the residual FSI behaves in a U(3) symmetric case. It is known that the $U_A(1)$ breaking is responsible for the mass difference between η and η' and U(3) symmetry is not a good symmetry for low-lying pseudoscalars. However, U(3) symmetry may still be a reasonable one for a system that rescatters at energies of order m_B. The mass difference between η and η', as an indicator of U(3) symmetry breaking effect, does not lead to sizable energy difference of these particles in charmless B decays. In the literature, some authors also make use of U(3) symmetry in charmless B decays (see, for example [36]).

The full U(3) symmetry requires

$$r_i=\bar{r}_i=\tilde{r}_i=\check{r}_i \quad (22)$$

for each $i=0,a,e,t$. This imposes a major reduction of parameters. Note that the reduction is more easier to preform in the r_i formalism than in the SU(3) decomposition formalism. This is one of the advantages of the former formalism.

In the U(3) case, we are constrained to have (see Appendix B)

$$r_e^{(m)}r_a^{(m)}=0. \quad (23)$$

Consequently, there are two different solutions: (a) the annihilation-type ($r_a^{(m)}\neq 0$, $r_e^{(m)}=0$) with

$$\delta_{27}=\delta_8'=\delta_1',\qquad \delta_8,\delta_1,\tau=-\frac{1}{2}\sin^{-1}\frac{4\sqrt{5}}{9},\qquad \nu=-\frac{1}{2}\sin^{-1}\frac{4\sqrt{2}}{9}, \quad (24)$$

and (b) the exchange-type ($r_e^{(m)}\neq 0$, $r_a^{(m)}=r_t^{(m)}=0$) with

$$\delta_{27}=\delta_8'=\delta_1',\qquad \delta_8=\delta_1,\qquad \tau=\frac{1}{2}\sin^{-1}\frac{\sqrt{5}}{3},\qquad \nu=\frac{1}{2}\sin^{-1}\frac{2\sqrt{2}}{3}. \quad (25)$$

The explicit expressions of $r_i^{(m)}$ in terms of these phases can be found in Appendix B.

It is interesting to note that in both solutions of the U(3) case, a common constraint

$$\delta_{27}=\delta_8'=\delta_1' \quad (26)$$

has to be satisfied. To reduce the number of the residual FSI parameters shown in Eq. (21), we consider a restricted SU(3) case, which is close, but not necessarily identical, to the full U(3) case. Motivated by Eq. (26), we consider the parameter space around

$$\delta'\simeq\sigma'\simeq 0,\qquad \kappa'\simeq\xi'\simeq 0. \quad (27)$$

The above restriction on the FSI parameter space is a rather strong model assumption. When comparing the fitted FSI

parameters with those in Eqs. (24) and (25), it is possible to determine whether the exchange-type, the annihilation-type, or a mixed solution is preferred by data.

III. NUMERICAL RESULTS

In our numerical study, masses and lifetimes are taken from the review of the Particle Data Group (PDG) [1], and the branching ratios of B to charmless meson decays are taken from [2,37,38]. We use $f_\pi = 131$ MeV, $f_K = 156$ MeV [1], and $f_{B_{(s)}} = 200(230)$ MeV for decay constants. The values of CKM matrix elements are taken from the central values of the latest CKMfitter's results [39].

We use the QCD factorization calculated amplitudes [24] for the factorization amplitudes in the right-hand side of Eq. (4). We take the renormalization scale $\mu = 4.2$ GeV and the power correction parameters $X_{A,H} = \ln(m_B/\Lambda_h)(1 + \rho_{A,H}e^{i\phi_{A,H}})$. Hadronic parameters in factorization amplitudes are fit parameters in addition to FSI parameters, and are allowed to vary in the following ranges:

$$\begin{aligned} &0 \le \rho_A = \rho_H \le 2, \qquad -\pi < \phi_{A,H} \le \pi, \\ &m_s(2.1\ \text{GeV}) = (100 \pm 30)\ \text{MeV}, \\ &F_0^{B\pi}(0) = 0.25 \pm 0.05, \qquad F_0^{BK}(0) = 0.35 \pm 0.08, \\ &F^{B_sK}(0) = 0.31 \pm 0.08. \end{aligned} \tag{28}$$

Note that we take $\rho_A = \rho_H$ for simplicity. These estimations agree with those in [24,40,41], while the ranges of form factors are slightly enlarged to include the possible effect of the overall scaling factor $\exp(-\text{Im}\delta_{27})$ from $\mathcal{S}_{\text{res}}^{1/2}$. Other parameters (if not specified explicitly) in the QCDF amplitudes are taken from the central values of those used in [24]. For the FSI parameters, we set allowed ranges to be

$$\begin{aligned} &-\frac{\pi}{2} < \tau, \nu \le \frac{\pi}{2}, \qquad -\pi < \delta, \sigma \le \pi, \\ &-0.35 \le \kappa, \xi \le 0.35 \end{aligned} \tag{29}$$

for the mixing angles, real and imaginary parts of FSI phase differences. In the fit we take $\delta' = \sigma' = \kappa' = \xi' = 0$ as mentioned in the end of the previous section. The effects of relaxing these constraints will also be estimated.

We perform a χ^2 analysis with all available data on CP-averaged rates and CP asymmetries in $\bar{B}_{u,d,s} \to PP$ decays. There are altogether 43 data used in the fit. The confidence level and χ^2 for the best-fitted case are shown in Table I. Contributions to χ^2_{min} from various subsets of data are also given. For example, $\chi^2_{\{\mathcal{B}(\bar{B}^0\to K\pi),\ldots\}}$ in the table denotes the χ^2 contribution obtained from 4 CP-averaged $\bar{B}^0 \to K^-\pi^+$, $\bar{K}^0\pi^0$, $\bar{K}^0\eta$, $\bar{K}^0\eta'$ rates, which are related through FSI [see Eq. (5), and see Eqs. (6)–(8) for other groups]. Numbers of data used are shown in parentheses.

From Table I, by comparing the χ^2 value and the number of data used in each group, we are able to have a rough idea on the quality of the fit. In most cases, the χ^2 values are compatible or smaller than the numbers of data used, indicating reasonable fit to measurements in these groups. However, the $\chi^2_{\{\mathcal{A}(B^-\to K\pi),\ldots\}}$, $\chi^2_{\{\mathcal{A}(B^-\to\pi\pi),\ldots\}}$ and $\chi^2_{S(\bar{B}^0)}$ values are larger than the corresponding numbers of data used. We will discuss more on the sources causing these sizable χ^2 later.

We give the fitted parameters in Table II. Uncertainties are obtained by scanning the parameter space with $\chi^2 \le \chi^2_{\text{min}} + 1$. The parameters consist of those in factorization amplitude (in the upper table) and of FSI (in the lower table). Values given in parenthesis are not fitted ones. We take δ', $\sigma' = (0 \pm 10)°$ and κ', $\xi' = 0 \pm 0.05$ for estimation.

We note that (i) Most of our fitted values for hadronic parameters in factorization amplitudes agree with those usually used in [24,40,41]. However, the fit seems to prefer

TABLE I. Confidence level, χ^2_{min}/d.o.f. and various contributions to χ^2_{min} for the best-fitted solution. Numbers of data used are shown in parentheses.

Confidence level	χ^2_{min}/d.o.f.	$\chi^2_{\{\mathcal{B}(\bar{B}^0\to K\pi),\ldots\}}$	$\chi^2_{\{\mathcal{A}(\bar{B}^0\to K\pi),\ldots\}}$	$\chi^2_{\{\mathcal{B}(B^-\to K\pi),\ldots\}}$	$\chi^2_{\{\mathcal{A}(B^-\to K\pi),\ldots\}}$
0.04 (43)	1.51 (43)	4.6 (4)	1.6 (3)	4.5 (4)	7.0 (4)
$\chi^2_{\{\mathcal{B}(B^-\to\pi\pi),\ldots\}}$	$\chi^2_{\{\mathcal{A}(B^-\to\pi\pi),\ldots\}}$	$\chi^2_{\{B(\bar{B}^0\to\pi\pi),\ldots\}}$	$\chi^2_{\{\mathcal{A}(\bar{B}^0\to\pi\pi),\ldots\}}$	$\chi^2_{\{\mathcal{B}(\bar{B}_s),\mathcal{A}(\bar{B}_s)\}}$	$\chi^2_{\{S(\bar{B}^0)\}}$
2.6 (4)	6.8 (4)	8.0 (9)	2.4 (3)	1.6 (4)	6.0 (4)

TABLE II. Fitted hadronic and FSI parameters. Upper table contains fitted parameters in factorization amplitudes, while the lower one contains fitted FSI parameters. Note that parameters with values given in parentheses are not fitted ones (see text).

$\rho_{A,H}$	$\phi_A(°)$	$\phi_H(°)$	m_s (MeV)	$F_0^{B\pi}(0)$	$F_0^{BK}(0)$	$F_0^{B_sK}(0)$	
$1.18^{+0.08}_{-0.23}$	$-65.7^{+16.3}_{-16.0}$	$7.5^{+40.6}_{-80.1}$	$84.3^{+1.8}_{-1.5}$	$0.258^{+0.017}_{-0.004}$	$0.314^{+0.030}_{-0.012}$	$0.237^{+0.025}_{-0.007}$	
$\tau(°)$	$\nu(°)$	$\delta(°)$	$\sigma(°)$	κ	ξ	δ', $\sigma'(°)$	κ', ξ'
$20.6^{+1.9}_{-1.8}$	$41.2^{+24.7}_{-3.8}$	$51.4^{+9.8}_{-26.8}$	$88.9^{+109.5}_{-8.9}$	$-0.35^{+0.03}_{-0.00}$	$0.26^{+0.09}_{-0.61}$	(0 ± 10)	(0 ± 0.05)

a small value of $F^{B_s K}(0)$, which is at the lower end of the allowed region given in Eq. (28). (ii) Although it helps improve the fit, the effect of ϕ_H is subleading. On the other hand, the effect of ϕ_A is prominent. The fitted ϕ_A is around $-66°$, which is close to $-55°$ as used in the so-called S4 scenario in QCDF [24]. When turning off FSI phases, our results should be similar to those obtained in the S4 scenario. (iii) The fitted $\tau \simeq 21°$ and $\nu \simeq 41°$ are closer to $\tau = 24.1°$ and $\nu = 35.3°$ of the exchange-type solution [see Eq. (25)] than to $\tau = -41.8°$ and $\nu = -19.5°$ of the annihilation-type solution [see Eq. (24)]. The exchange-type solution is more favorable. (iv) In this work, residual FSI is taken as leftover FSI that complements the FSI in factorization amplitudes. In principle, there is a possible double counting in $\phi_{A,H}$ and residual FSI phases. However, in practice the residual FSI is dominated by the exchange rescattering, which provides important effects on rates and CP asymmetries as we shall see later. These effects cannot be easily obtained by varying $\rho_{A,H}$ and $\phi_{A,H}$ in reasonable ranges. In fact, numerically the χ^2/d.o.f. will not be reduced by freezing either of these parameters. Hence, both parameters are numerically important.

A. Rates in $\bar{B}^0$ and B^- decays

In Table III, we show the CP-average rates of $\bar{B}^0$, $B^- \to PP$ decays. In the table, Fac, "FSI," and FSI denote factorization, partial FSI, and full FSI results, respectively. The FSI results are obtained with the best-fitted parameters shown in Table II. The factorization results are obtained by using the same set of the best-fitted parameters, but with the residual FSI phases ($\delta^{(\prime)}$, $\sigma^{(\prime)}$, $\kappa^{(\prime)}$, and $\xi^{(\prime)}$) set to zero, while the partially FSI results are obtained similarly, but only with the real FSI phases ($\delta^{(\prime)}$, $\sigma^{(\prime)}$) set to zero. Recall that in Eq. (20) the $\mathcal{S}^{1/2}_{\rm res}$ matrix can be factorized into two parts, one involving real FSI phases and the other involving imaginary phases. The "FSI" results only make use of the one involving imaginary phases and are sort of "halfway" from the factorization results to the full FSI ones.

Uncertainties for factorization results are not given and can be found elsewhere (for example, in [24]). The first uncertainties in FSI results are obtained by scanning the parameter space with $\chi^2 \le \chi^2_{\rm min} + 1$, while keeping $\delta' = \sigma' = 0$ and $\kappa' = \xi' = 0$. The second uncertainties in FSI results are from the variations of δ', σ', κ', and ξ'. From the table, we see that the $\bar{B} \to \bar{K}\pi$ and $\bar{B} \to \bar{K}\eta^{(\prime)}$ rates are quite sensitive to δ', σ', κ', and ξ'. Hence, a larger variation of these parameters is not preferred by the data.

As shown in Table III, the residual FSI results agree with data. Before turning on the residual FSI, the factorization results are close to the S4 ones as expected. After the residual FSI is turned on, some rates are enhanced remarkably. In particular, $\bar{B}^0$ decays in the $\Delta S = 0$ transitions receive large contributions from the residual FSI. In the following, we will focus on effects of the FSI on some interesting modes.

TABLE III. Branching ratios of various $\bar{B} \to PP$ modes in units of 10^{-6}. Fac, "FSI," and FSI denote factorization, partial FSI and full FSI results, respectively. See the main text for details. Experimental results are taken from [2,37].

Mode	Exp	Fac	"FSI"	FSI
$\bar{B}^0 \to K^- \pi^+$	19.4 ± 0.6	(16.0)	(22.5)	$20.1^{+1.7+2.5}_{-0.3-2.5}$
$\bar{B}^0 \to \bar{K}^0 \pi^0$	9.8 ± 0.6	(7.2)	(10.2)	$9.2^{+0.7+1.2}_{-0.2-1.2}$
$\bar{B}^0 \to \bar{K}^0 \eta$	1.0 ± 0.3	(0.9)	(1.7)	$1.4^{+0.4+0.5}_{-0.1-0.4}$
$\bar{B}^0 \to \bar{K}^0 \eta'$	64.9 ± 3.1	(66.4)	(62.3)	$65.9^{+6.9+9.2}_{-10.6-8.1}$
$B^- \to \bar{K}^0 \pi^-$	23.1 ± 1.0	(18.0)	(26.1)	$22.5^{+2.6+3.0}_{-1.1-0.7}$
$B^- \to K^- \pi^0$	12.9 ± 0.6	(10.1)	(14.3)	$12.4^{+1.5+1.6}_{-0.2-1.6}$
$B^- \to K^- \eta$	2.7 ± 0.3	(1.4)	(2.5)	$2.1^{+0.6+0.6}_{-0.1-0.5}$
$B^- \to K^- \eta'$	70.2 ± 2.5	(70.1)	(65.0)	$70.8^{+6.6+10.3}_{-12.3-9.2}$
$B^- \to \pi^- \pi^0$	$5.59^{+0.41}_{-0.40}$	(5.18)	(5.18)	$5.18^{+0.55+0.00}_{-0.38-0.00}$
$B^- \to K^0 K^-$	$1.36^{+0.29}_{-0.27}$	(1.22)	(1.77)	$1.46^{+0.35+0.15}_{-0.04-0.13}$
$B^- \to \pi^- \eta$	4.4 ± 0.4	(4.10)	(4.47)	$4.23^{+0.59+0.34}_{-0.23-0.37}$
$B^- \to \pi^- \eta'$	$2.7^{+0.6}_{-0.5}$	(3.09)	(2.76)	$3.31^{+0.19+0.65}_{-0.51-0.54}$
$\bar{B}^0 \to \pi^+ \pi^-$	5.16 ± 0.22	(6.65)	(7.56)	$5.30^{+1.92+0.39}_{-0.49-0.40}$
$\bar{B}^0 \to \pi^0 \pi^0$	1.55 ± 0.35[a]	(0.50)	(0.36)	$1.04^{+0.12+0.10}_{-0.55-0.08}$
$\bar{B}^0 \to \eta \eta$	$0.8 \pm 0.4 (<1.4)$	(0.21)	(0.10)	$0.46^{+0.24+0.10}_{-0.11-0.08}$
$\bar{B}^0 \to \eta \eta'$	$0.5 \pm 0.4 (<1.2)$	(0.22)	(0.24)	$0.88^{+0.39+0.24}_{-0.40-0.21}$
$\bar{B}^0 \to \eta' \eta'$	$0.9^{+0.8}_{-0.7} (<2.1)$	(0.16)	(0.30)	$1.06^{+1.16+0.36}_{-0.31-0.28}$
$\bar{B}^0 \to K^+ K^-$	$0.15^{+0.11}_{-0.10}$	(0.09)	(0.05)	$0.10^{+0.35+0.10}_{-0.02-0.06}$
$\bar{B}^0 \to K^0 \bar{K}^0$	$0.96^{+0.21}_{-0.19}$	(1.47)	(1.56)	$1.10^{+0.46+0.12}_{-0.12-0.11}$
$\bar{B}^0 \to \pi^0 \eta$	$0.9 \pm 0.4 (<1.5)$	(0.26)	(0.37)	$0.31^{+0.05+0.06}_{-0.01-0.06}$
$\bar{B}^0 \to \pi^0 \eta'$	1.2 ± 0.7[b]	(0.32)	(0.22)	$0.42^{+0.02+0.13}_{-0.15-0.11}$

[a] An S factor of 1.8 is included in the uncertainty.
[b] An S factor of 1.7 is included in the uncertainty.

Through the residual FSI, $\bar{B}^0 \to \pi^+ \pi^-$ and $\pi^0 \pi^0$ rates[2] are reduced and enhanced roughly by factor 2, respectively, leading to a better agreement with data. Note that in the "FSI" case, the $\pi^+ \pi^-$ rate is enhanced, while the $\pi^0 \pi^0$ rate is slightly reduced. Both of them are pushed even further from the data. There are the real FSI phases (δ, σ) that will change these rates in the right direction.

In Fig. 2, we show the $\bar{B}^0 \to \pi^+ \pi^-$ and $\pi^0 \pi^0$ rates versus δ. The solid line is obtained by using all other parameters set to their best-fitted values, while the dashed line is obtained using the exchange-type solution for FSI parameters [see, Eq. (25)] with τ, ν fixed, $\sigma = \delta$ and $\kappa = \xi$ taken from the average of the central values of the fitted κ and ξ. We see that $\bar{B}^0 \to \pi^+ \pi^-$ and $\pi^0 \pi^0$ rates are reduced and enhanced, respectively, as δ is increasing. Both rates reach the measured ones at $\delta \sim 0.3\pi$.

[2] For the factorization amplitudes, we use the central values of Gegenbauer coefficients for the pion wave function, $\alpha_2^\pi(2\ {\rm GeV}) = 0.2 \pm 0.1$, used in [42] and do not consider the case of using a larger Gegenbauer coefficient, which leads to a larger $\pi^0 \pi^0$ rate.

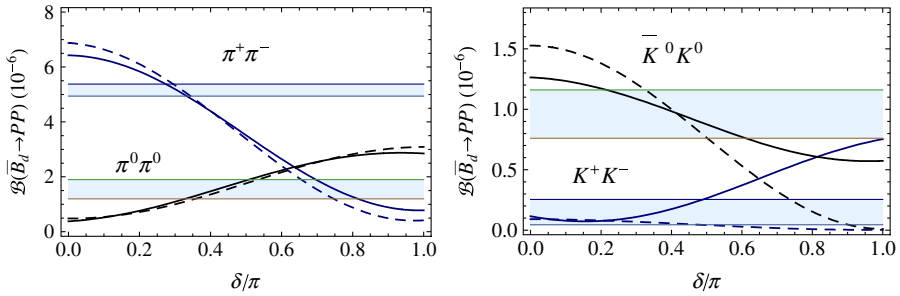

FIG. 2 (color online). $\bar{B}^0 \to \pi^+\pi^-$, $\pi^0\pi^0$ rates (left) and $\bar{B}^0 \to K^+K^-$, $\bar{K}^0K^0$ rates (right) versus δ are plotted. The solid line is obtained by using all other parameters set to their best-fitted values, while the dashed line is obtained using the exchange-type solution for FSI parameters (see text). Bands are one-sigma ranges of experimental data. Theoretical uncertainties are not shown. Note that the fitted δ/π is around 0.3 (see Table II).

It is known that in order to have the $\pi^0\pi^0$ rate as large as observed, we need a sizable color-suppressed tree amplitude [43]. In the residual FSI, a large color-suppressed tree contribution can be generated from the exchange rescattering. As shown in the upper part of Fig. 3, the color-allowed tree amplitude of the $\bar{B}^0 \to \pi^+\pi^-$ decay, a main FSI source in this sector, can produce a color-suppressed tree amplitude for the $\bar{B}^0 \to \pi^0\pi^0$ decay through the exchange rescattering. At the same time, the $\pi^+\pi^-$ rate is reduced as it rescatters. We see that the exchange rescattering is responsible for the enhancement of $\pi^0\pi^0$ and the suppression of $\pi^+\pi^-$.

In Fig. 2, we show the $\bar{B}^0 \to K^+K^-$ and $\bar{K}^0K^0$ rates. It is known that the K^+K^- rate is sensitive to annihilation-type rescattering [27] (corresponding to the r_a and r_t terms as depicted in Fig. 1(c) and 1(d)). In the SU(3) case (solid line), for $\delta \leq \pi/2$, the K^+K^- constraint can be easily satisfied, while in the U(3) case (dashed line), the constraint on δ is even weaker. These features are understandable, since in both cases, the exchange-type rescattering, which cannot generate K^+K^- final state by rescattering the $\bar{B}^0 \to \pi^+\pi^-$ decay amplitude, is dominating. Note that the $\bar{K}^0K^0$ rate is reduced through FSI, giving better agreement with data without violating the K^+K^- bound.

In summary, the residual FSI improves the agreement between theory and experiment for rates, in particular, it resolves the discrepancy between data and theoretical expectations on $\bar{B}^0 \to \pi^+\pi^-$ and $\pi^0\pi^0$ rates.

B. Direct *CP* violations in $\bar{B}^0$ and B^- decays

Results for direct *CP* asymmetries in $\bar{B}^0$, $B^- \to PP$ decays are summarized in Table IV. In general, the residual FSI has a large impact on direct *CP* violations of many modes. In the following, we will focus on some interesting results.

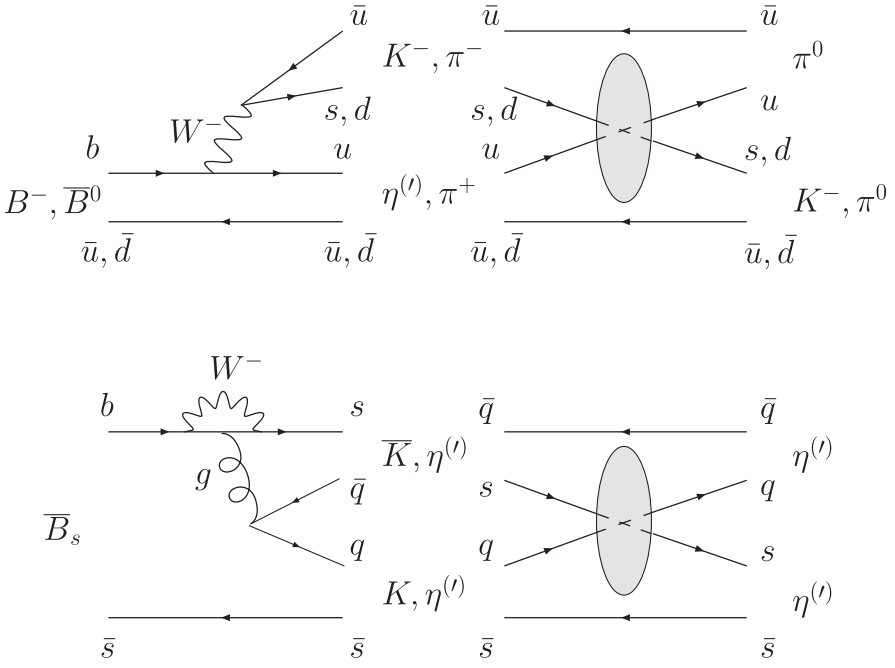

FIG. 3. Exchange rescattering in $\bar{B}^0 \to \pi^0\pi^0$, $B^- \to K^-\pi^0$, and $\bar{B}_s \to \eta^{(\prime)}\eta^{(\prime)}$ decays.

TABLE IV. Same as Table III, except for the direct CP asymmetries $\mathcal{A}$ (in units of percent) in various $\bar{B} \to PP$ modes.

Mode	Exp	Fac	"FSI"	FSI
$\bar{B}^0 \to K^- \pi^+$	$-9.8^{+1.2}_{-1.1}$	(-11.8)	(-12.2)	$-9.0^{+2.0+2.0}_{-0.6-2.2}$
$\bar{B}^0 \to \bar{K}^0 \pi^0$	-1 ± 13^{a}	(3.3)	(0.9)	$-12.8^{+2.2+1.7}_{-1.0-1.5}$
$\bar{B}^0 \to \bar{K}^0 \eta$	-	(10.7)	(2.1)	$-28.7^{+8.0+3.3}_{-1.9-1.9}$
$\bar{B}^0 \to \bar{K}^0 \eta'$	4.8 ± 5.1	(0.2)	(0.6)	$1.7^{+0.8+0.3}_{-0.2-0.4}$
$B^- \to \bar{K}^0 \pi^-$	0.9 ± 2.5	(0.3)	(0.2)	$-0.3^{+0.7+1.2}_{-0.6-1.1}$
$B^- \to K^- \pi^0$	5.0 ± 2.5	(-11.8)	(-10.3)	$4.8^{+1.4+1.9}_{-1.2-2.0}$
$B^- \to K^- \eta$	-27 ± 9	(39.8)	(28.2)	$-27.3^{+8.6+10.8}_{-3.0-6.3}$
$B^- \to K^- \eta'$	1.6 ± 1.9	(-2.6)	(-2.6)	$-3.3^{+1.0+0.5}_{-0.5-0.5}$
$B^- \to \pi^- \pi^0$	6 ± 5	(-0.06)	(-0.06)	$-0.06^{+0.00+0.00}_{-0.01-0.00}$
$B^- \to K^0 K^-$	12^{+17}_{-18}	(-3.5)	(-1.8)	$12.8^{+9.1+16.0}_{-12.8-17.8}$
$B^- \to \pi^- \eta$	-16 ± 7	(19.7)	(22.0)	$-12.3^{+4.1+3.5}_{-2.9-3.2}$
$B^- \to \pi^- \eta'$	21 ± 15	(22.8)	(20.3)	$54.8^{+5.3+1.7}_{-10.6-3.0}$
$\bar{B}^0 \to \pi^+ \pi^-$	38 ± 15^{b}	(22.3)	(21.1)	$15.5^{+10.2+4.6}_{-4.3-4.5}$
$\bar{B}^0 \to \pi^0 \pi^0$	43^{+25}_{-24}	(-51.5)	(-45.8)	$48.3^{+11.5+11.8}_{-33.1-13.1}$
$\bar{B}^0 \to \eta \eta$	-	(-11.7)	(-77.6)	$-50.7^{+15.0+15.7}_{-12.4-16.3}$
$\bar{B}^0 \to \eta \eta'$	-	(-28.5)	(-29.3)	$-5.7^{+9.5+7.8}_{-22.2-7.4}$
$\bar{B}^0 \to \eta' \eta'$	-	(3.6)	(18.7)	$29.7^{+26.2+8.3}_{-1.7-6.6}$
$\bar{B}^0 \to K^+ K^-$	-	(0)	(52.9)	$71.0^{+10.9+20.6}_{-41.4-15.6}$
$\bar{B}^0 \to K^0 \bar{K}^0$	-58^{+73}_{-66}	(-9.0)	(-19.9)	$-37.8^{+8.4+15.2}_{-37.1-15.0}$
$\bar{B}^0 \to \pi^0 \eta$	-	(19.7)	(19.1)	$7.2^{+11.5+0.4}_{-13.8-0.5}$
$\bar{B}^0 \to \pi^0 \eta'$	-	(13.2)	(12.4)	$22.7^{+7.7+1.0}_{-20.5-1.0}$

[a]An S factor of 1.4 is included in the uncertainty.
[b]An S factor of 2.4 is included in the uncertainty.

We first concentrate on the modes that lead to the $K\pi$ puzzle in direct CP violation. We see that before the residual FSI is turned on (i.e. taking $\mathcal{S}_{\rm res} = 1$), we have $\mathcal{A}(\bar{B}^0 \to K^- \pi^+) \simeq \mathcal{A}(B^- \to K^- \pi^0) \simeq -0.12$ from the annihilation amplitude for $\phi_A (\simeq -66°)$. After turning on the residual FSI ($\mathcal{S}_{\rm res} \neq 1$), the asymmetry $\mathcal{A}(\bar{B}^0 \to K^- \pi^+)$ changes from ~ -0.12 to ~ -0.09, while $\mathcal{A}(B^- \to K^- \pi^0)$ changes from ~ -0.12 to $\sim +0.05$, reproducing the experimental results. In other words, the residual FSI modifies $\mathcal{A}(\bar{B}^0 \to K^- \pi^+)$ and $\mathcal{A}(B^- \to K^- \pi^0)$ by an amount of $\sim +0.03$ and $\sim +0.17$, respectively.

The residual FSI has a more prominent effect on $\mathcal{A}(B^- \to K^- \pi^0)$, and, hence, it is capable of lifting the degeneracy of $\mathcal{A}(B^- \to K^- \pi^0)$ and $\mathcal{A}(\bar{B}^0 \to K^- \pi^+)$. As shown in Fig. 4, it only takes a small amount of δ ($\sim 0.2\pi$) to flip the sign of $\mathcal{A}(B^- \to K^- \pi^0)$, but a large δ ($\gtrsim 0.8\pi$) would be needed to do the same thing on $\mathcal{A}(\bar{B}^0 \to K^- \pi^+)$.

It is known that a sizable and complex color-suppressed tree amplitude in the $B^- \to K^- \pi^0$ decay can solve the $K\pi$ puzzle [43]. As depicted in Fig. 3, a color-suppressed tree amplitude in the $K^- \pi^0$ mode can be generated from the exchange rescattering of $B^- \to K^- \eta^{(\prime)}$ color-allowed tree amplitudes, which are known to be quite sizable [24]. The rescattering leads to the desired large and complex color-suppressed amplitude in the $K^- \pi^0$ mode.

We note that in order to solve the $K\pi$ direct CP puzzle, both ϕ_A and δ phases are needed. For example, a similar analysis using rescattering among naive factorization amplitudes that lack a large annihilation strong phase, was unable to remove the degeneracy of $\mathcal{A}(K^- \pi^+)$ and $\mathcal{A}(K^- \pi^0)$ [27]. In other words, rescattering from both inelastic channels and PP final states contribute to $\mathcal{A}(\bar{K}\pi)$s, reproducing the experimental results and resolving the $K\pi$ direct CP-violation puzzle without the need of introducing any new physics contribution.

As noted in the previous section, the exchange rescattering is also responsible for the enhancement of the $\bar{B}^0 \to \pi^0 \pi^0$ rate. In Fig. 5, we show a two-dimensional plot, exhibiting the correlation of the ratio $\mathcal{B}(\bar{B}^0 \to \pi^0 \pi^0)/\mathcal{B}(\bar{B}^0 \to \pi^+ \pi^-)$ with the difference $\Delta\mathcal{A} \equiv \mathcal{A}(\bar{B}^0 \to K^- \pi^+) - \mathcal{A}(B^- \to K^- \pi^0)$. The light shaded area is obtained by scanning over $-\pi < \delta, \sigma \leq \pi$ and one-sigma ranges of τ, ν, κ, and ξ, while keeping all other hadronic parameters at their best-fitted values. The dark shaded area corresponds to the exchange-type U(3) case and is obtained by scanning over $-\pi < \delta = \sigma \leq \pi$, $-0.35 \leq \kappa = \xi \leq 0.35$, while using τ and ν given in Eq. (25) and keeping all other hadronic parameters at their best-fitted values. The solid line is obtained in a similar manner except keeping $\kappa = \xi = -0.05$, which is the average of the central values of the best-fitted κ and ξ. Note that in this case, only one FSI parameter δ is varied. From the plot, we clearly see that the data can be easily repro-

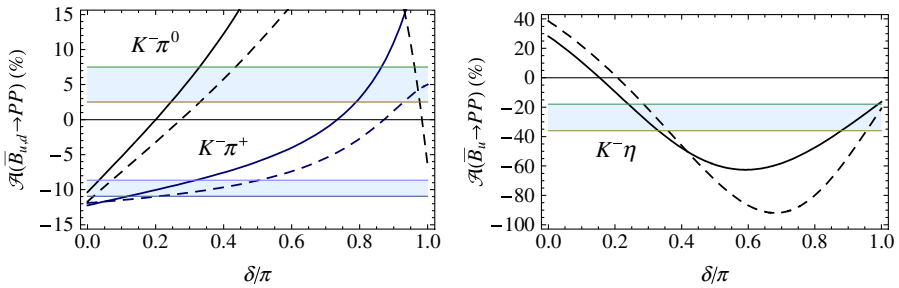

FIG. 4 (color online). Same as Fig. 2, except that direct CP violations of $\bar{B}^0 \to K^- \pi^+$ and $B^- \to K^- \pi^0$ (left), and $\bar{B}^0 \to K^- \eta$ (right) versus δ are plotted. Note that the best-fitted δ/π is around 0.3.

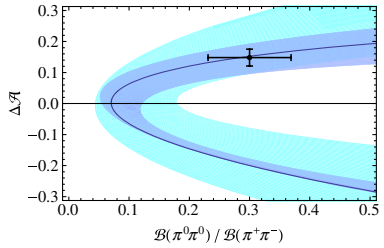

FIG. 5 (color online). Correlation of the ratio $\mathcal{B}(\bar{B}^0 \to \pi^0\pi^0)/\mathcal{B}(\bar{B}^0 \to \pi^+\pi^-)$ with the difference $\Delta\mathcal{A} \equiv \mathcal{A}(K^-\pi^+) - \mathcal{A}(K^-\pi^0)$. The light shaded area corresponds to the restricted SU(3) case, the dark shaded area corresponds to the exchange-type U(3) case and the solid line is the same as the previous one except keeping $\kappa = \xi = -0.05$. See the main text for more details.

duced, and the exchange rescattering is responsible for generating sizable and complex color-suppressed tree amplitudes that account for the difference $\Delta\mathcal{A}$ and the $\mathcal{B}(\bar{B}^0 \to \pi^0\pi^0)/\mathcal{B}(\bar{B}^0 \to \pi^+\pi^-)$ ratio at the same time.

We now continue to discuss FSI effects on direct CP asymmetries. There are several interesting results and remarks: (i) Large effects of residual FSI on $\mathcal{A}$ for several other modes are obtained. Direct CP asymmetries in $\bar{B}^0 \to \bar{K}^0\pi^0, \bar{K}^0\eta, \pi^0\pi^0$ decays and in $B^- \to K^-\pi^0, K^-\eta, \pi^-\eta$ decays change signs in the presence of FSI. In Fig. 4, we see that $\mathcal{A}(B^- \to K^-\eta)$ is quite sensitive to FSI. The solid line passes through the one-sigma range of data around $\delta \sim 0.3\pi$. (ii) Recall that in Table I, we have $\chi^2_{\{\mathcal{A}(B^-\to K\pi),\ldots\}} = 7.0$ and $\chi^2_{\{\mathcal{A}(B^-\to\pi\pi),\ldots\}} = 6.8$ from $\mathcal{A}(B^- \to \bar{K}^0\pi^-, K^-\pi^0, K^-\eta, K^-\eta')$ and $\mathcal{A}(B^- \to \pi^-\pi^0, K^0K^-, \pi^-\eta, \pi^-\eta')$ results, respectively. We see from Table IV that the main contributions to these χ^2 are from $\mathcal{A}(B^- \to K^-\eta')$ and $\mathcal{A}(B^- \to \pi^-\eta')$, respectively. (iii) Note that the experimental uncertainty of $\mathcal{A}(\bar{B}^0 \to \pi^+\pi^-)$ is enlarged by a PDG S factor originated from two different measurements: $0.25 \pm 0.08 \pm 0.02$ and $0.55 \pm 0.08 \pm 0.05$ from BABAR [37] and Belle [44], respectively. Our fitted result of $\mathcal{A}(\bar{B}^0 \to \pi^+\pi^-) = (15.5^{+10.2+4.6}_{-4.3-4.5})\%$ prefers the BABAR data. (iv) The direct CP violation of $\bar{B}^0 \to \pi^0\pi^0$ flips its sign, resulting in a large and positive $\mathcal{A}(\pi^0\pi^0)$. (v) The direct CP violation of $B^- \to \pi^-\pi^0$ is very small and does not receive any contribution from the residual rescattering, since it can only rescatter into itself [see Eq. (7)]. The smallness of $\mathcal{A}(B^- \to \pi^-\pi^0)$ is consistent with a requirement followed from the CPT theorem [45]. The $\mathcal{A}(B^- \to \pi^-\pi^0)$ measurement remains as a clean way to search for new physics effects [22].

C. Rates and direct CP asymmetries in $\bar{B}^0_s$ decays

We now turn to B_s decays. In Table V, we show the CP-averaged rates and direct CP violations of $\bar{B}^0_s \to PP$ decays. The results are then compared with the data. From the table, we see that (i) The $\mathcal{B}(\bar{B}_s \to K^-\pi^+)$ rate agrees well with data. From Fig. 6, we note that the result is in agreement with the data for $0 < \delta < \pi/2$ and any value of σ. (ii) The $\mathcal{B}(\bar{B}_s \to K^+K^-)$ rate plotted in Fig. 6 versus δ and σ agrees with the data. (iii) The $\mathcal{B}(\bar{B}_s \to \pi^+\pi^-)$ data can be reproduced, but the result has a large uncertainty. (iv) The $\mathcal{A}(\bar{B}_s \to K^-\pi^+)$ data can be reproduced, but the fitted value is close to the lower end of the data.

We expect the residual FSI to have sizable contributions to various $\bar{B}_s \to PP$ decay rates. For example, from Fig. 3 we see that the $\bar{B}_s \to \eta^{(\prime)}\eta^{(\prime)}$ decays also receive contributions from the exchange rescattering. Plots of $\bar{B}_s \to \eta^{(\prime)}\eta^{(\prime)}$ rates versus δ and σ are shown in Fig. 6. The $\bar{B}_s \to \eta'\eta'$ rate is quite sensitive to the FSI phase σ. As shown in Table V, the $\bar{B}^0_s \to \eta'\eta'$ branching ratio is enhanced by a factor of 1.2 and reaches 1.0×10^{-4}, which can be checked in the near future. The $\bar{B}_s \to \bar{K}^0\pi^0$ and $\bar{K}^0\eta$ modes are also quite sensitive to the residual rescattering, and their rates are enhanced by factors of 1.5 to 2, respectively.

Similar to the $\bar{B}_{u,d}$ cases, the residual FSI also has a large impact on many $\mathcal{A}(\bar{B}_s \to PP)$. From Table V, we see that signs of $\mathcal{A}(\bar{B}_s \to \bar{K}^0\pi^0)$ and $\mathcal{A}(\bar{B}_s \to \bar{K}^0\eta')$ are flipped. Note that direct CP asymmetries in $\bar{B}_s \to \bar{K}^0\pi^0, \bar{K}^0\eta, \pi^0\eta$ and $\pi^0\eta'$ decays are close to or greater than 50%. On the contrary, direct CP asymmetries in penguin dominated $b \to s$ transition modes, such as $\bar{B}_s \to K^0\bar{K}^0$, $\eta\eta'$ and $\eta'\eta'$ decays, are predicted to be quite small. It should be noted that these results may be subject to some small SU(3) breaking effects.

There is increasing interest in the $\bar{B}_s$ sector [1,23]. It is expected that more data from CDF and other detectors should be available soon. Predictions on $\bar{B}_s$ decay rates and direct CP violations given here can be tested in the near future.

D. Time-dependent CP violations in $\bar{B}^0$ and $\bar{B}^0_s$ decays

Results on time-dependent CP asymmetries S are given in Table VI. The sources of the first two uncertainties are the same as those in previous tables, while the last uncertainty comes from the variation of $\gamma/\phi_3 = (67.6^{+2.8}_{-4.5})^\circ$ [39]. We fit to data on mixing induced CP asymmetries. Note that for the $\bar{B}^0 \to K^0\bar{K}^0$ mode, the mixing induced CP asymmetry obtained by BABAR ($-1.28^{+0.80+0.11}_{-0.73-0.16}$ [46]) and Belle ($-0.38^{+0.69}_{-0.77} \pm 0.08$ [47]) are quite different, and the central value of the former exceeds the physical range. Consequently, for this mode, only the Belle result is used in our fit.

Time-dependent CP asymmetries S of most $\bar{B}^0$ decay modes, except $\bar{B}^0 \to \pi^0\pi^0$, $\eta\eta$, K^+K^-, and $K^0\bar{K}^0$ decays, do not receive large contributions from the residual FSI. Likewise, S_f in most of $\bar{B}_s$ modes are not sensitive to FSI effects, except those in $\bar{B}^0_s \to \pi^0\eta^{(\prime)}$, $K_S\pi^0$, and $K_S\eta^{(\prime)}$ decays.

For $\bar{B}^0$ decays, we define $\Delta S \equiv \sin 2\beta_{\rm eff} - \sin 2\beta_{c\bar{c}K}$, where $\sin 2\beta_{\rm eff} = -\eta_f S(f)$ with η_f the CP eigenvalue

TABLE V. Same as Table III, except for the branching ratios (upper table) in the unit of 10^{-6} and direct CP asymmetries (lower table) in the unit of percent for various $\bar{B}_s \to PP$ modes. Experimental results are from [2,38].

Mode	Exp	Fac	"FSI"	FSI
$\mathcal{B}(\bar{B}_s^0 \to K^-\pi^+)$	5.00 ± 1.25	(4.72)	(6.08)	$4.81^{+1.57+0.20}_{-0.39-0.22}$
$\mathcal{B}(\bar{B}_s^0 \to \bar{K}^0\pi^0)$	-	(0.68)	(0.59)	$1.13^{+0.24+0.05}_{-0.33-0.04}$
$\mathcal{B}(\bar{B}_s^0 \to \bar{K}^0\eta)$	-	(0.28)	(0.21)	$0.59^{+0.10+0.04}_{-0.16-0.04}$
$\mathcal{B}(\bar{B}_s^0 \to \bar{K}^0\eta')$	-	(2.33)	(2.11)	$2.44^{+0.14+0.42}_{-0.44-0.36}$
$\mathcal{B}(\bar{B}_s^0 \to \pi^+\pi^-)$	0.53 ± 0.51	(0.30)	(0.10)	$0.86^{+1.72+2.93}_{-0.19-0.85}$
$\mathcal{B}(\bar{B}_s^0 \to \pi^0\pi^0)$	-	(0.15)	(0.05)	$0.43^{+0.86+1.47}_{-0.10-0.43}$
$\mathcal{B}(\bar{B}_s^0 \to \eta\eta)$	-	(17.5)	(21.3)	$20.2^{+7.6+5.9}_{-1.2-4.5}$
$\mathcal{B}(\bar{B}_s^0 \to \eta\eta')$	-	(70.8)	(65.7)	$63.6^{+47.1+13.7}_{-9.2-9.7}$
$\mathcal{B}(\bar{B}_s^0 \to \eta'\eta')$	-	(81.9)	(85.3)	$99.1^{+6.9+15.2}_{-72.3-13.4}$
$\mathcal{B}(\bar{B}_s^0 \to K^+K^-)$	24.4 ± 4.8	(24.7)	(25.3)	$20.7^{+11.5+3.3}_{-2.1-3.0}$
$\mathcal{B}(\bar{B}_s^0 \to K^0\bar{K}^0)$	-	(25.4)	(27.1)	$20.4^{+12.1+3.8}_{-1.8-3.4}$
$\mathcal{B}(\bar{B}_s^0 \to \pi^0\eta)$	-	(0.06)	(0.09)	$0.09^{+0.03+0.00}_{-0.00-0.00}$
$\mathcal{B}(\bar{B}_s^0 \to \pi^0\eta')$	-	(0.09)	(0.11)	$0.13^{+0.03+0.01}_{-0.00-0.01}$
$\mathcal{A}(\bar{B}_s^0 \to K^-\pi^+)$	39 ± 17	(33.4)	(36.7)	$26.6^{+2.7+4.8}_{-5.2-4.7}$
$\mathcal{A}(\bar{B}_s^0 \to \bar{K}^0\pi^0)$	-	(-49.1)	(-46.8)	$45.5^{+30.7+10.1}_{-12.6-10.5}$
$\mathcal{A}(\bar{B}_s^0 \to \bar{K}^0\eta)$	-	(2.0)	(-3.5)	$76.4^{+14.9+6.0}_{-5.1-7.7}$
$\mathcal{A}(\bar{B}_s^0 \to \bar{K}^0\eta')$	-	(2.5)	(-2.9)	$-14.6^{+4.3+5.7}_{-21.8-4.2}$
$\mathcal{A}(\bar{B}_s^0 \to \pi^+\pi^-)$	-	(0)	(-22.7)	$-6.1^{+9.7+56.4}_{-1.2-21.5}$
$\mathcal{A}(\bar{B}_s^0 \to \pi^0\pi^0)$	-	(0)	(-22.7)	$-6.1^{+9.7+56.4}_{-1.2-21.5}$
$\mathcal{A}(\bar{B}_s^0 \to \eta\eta)$	-	(1.6)	(1.1)	$-3.6^{+2.6+1.9}_{-1.6-1.4}$
$\mathcal{A}(\bar{B}_s^0 \to \eta\eta')$	-	(0.4)	(0.5)	$0.2^{+1.7+1.1}_{-0.1-1.0}$
$\mathcal{A}(\bar{B}_s^0 \to \eta'\eta')$	-	(0.2)	(0.0)	$0.0^{+0.2+0.4}_{-3.5-0.3}$
$\mathcal{A}(\bar{B}_s^0 \to K^+K^-)$	-	(-11.9)	(-12.7)	$-11.0^{+3.1+2.7}_{-1.3-2.9}$
$\mathcal{A}(\bar{B}_s^0 \to K^0\bar{K}^0)$	-	(0.3)	(1.1)	$2.2^{+1.8+1.2}_{-0.3-1.1}$
$\mathcal{A}(\bar{B}_s^0 \to \pi^0\eta)$	-	(3.9)	(4.7)	$82.8^{+5.5+4.2}_{-20.0-4.9}$
$\mathcal{A}(\bar{B}_s^0 \to \pi^0\eta')$	-	(37.5)	(33.5)	$93.9^{+2.7+3.2}_{-15.5-4.4}$

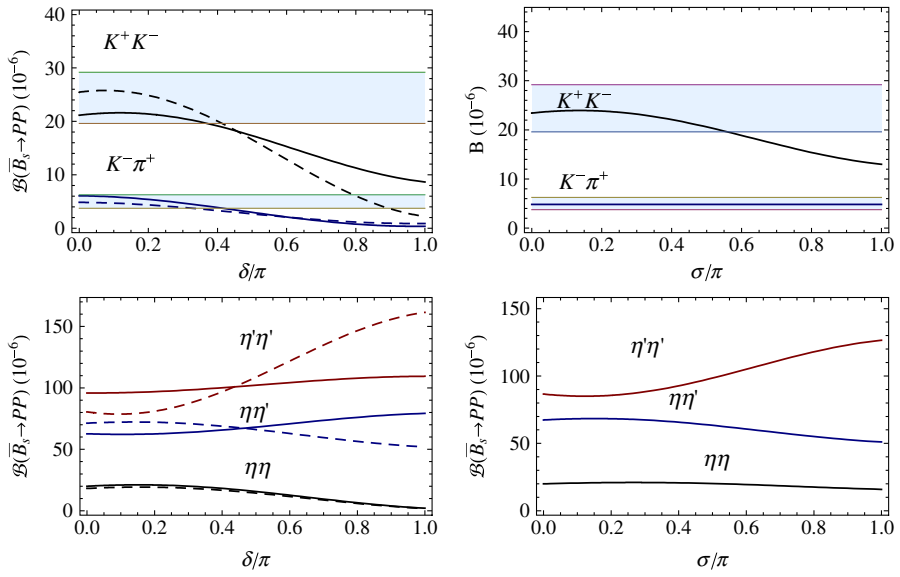

FIG. 6 (color online). Same as Fig. 2 except that $\bar{B}_s^0 \to K^-\pi^+$ and K^+K^- rates (top), $\bar{B}_s^0 \to \eta^{(\prime)}\eta^{(\prime)}$ rates (bottom) versus δ (left) or σ (right) [with all other parameters fixed at the best-fitted values] are plotted here. Theoretical uncertainties are not shown. Note that the best-fitted values for these FSI phases are $\delta/\pi \sim 0.3$ and $\sigma/\pi \sim 0.5$.

TABLE VI. Results on the time-dependent CP asymmetry S of various $\bar{B}_{d,s} \to PP$ modes. The first two uncertainties are same as those in previous tables, while the last uncertainty comes from the variation of γ/ϕ_3.

Mode	Exp	Fac	"FSI"	FSI
$\bar{B}^0 \to K_S\pi^0$	0.58 ± 0.17	(0.780)	(0.747)	$0.778^{+0.003+0.014+0.003}_{-0.037-0.013-0.002}$
$\bar{B}^0 \to K_S\eta$	-	(0.831)	(0.772)	$0.769^{+0.013+0.043+0.000}_{-0.050-0.039-0.001}$
$\bar{B}^0 \to K_S\eta'$	0.60 ± 0.07	(0.691)	(0.696)	$0.682^{+0.008+0.004+0.000}_{-0.002-0.004-0.000}$
$\bar{B}^0 \to \pi^+\pi^-$	-0.65 ± 0.07	(-0.591)	(-0.533)	$-0.542^{+0.088+0.038+0.139}_{-0.005-0.034-0.074}$
$\bar{B}^0 \to \pi^0\pi^0$	-	(0.854)	(0.820)	$0.484^{+0.425+0.096+0.145}_{-0.114-0.109-0.096}$
$\bar{B}^0 \to \eta\eta$	-	(-0.985)	(-0.378)	$-0.308^{+0.122+0.144+0.160}_{-0.237-0.110-0.089}$
$\bar{B}^0 \to \eta\eta'$	-	(-0.945)	(-0.956)	$-0.946^{+0.015+0.020+0.034}_{-0.036-0.016-0.016}$
$\bar{B}^0 \to \eta'\eta'$	-	(-0.901)	(-0.946)	$-0.917^{+0.089+0.030+0.001}_{-0.024-0.021-0.000}$
$\bar{B}^0 \to K^+K^-$	-	(-0.920)	(-0.468)	$-0.630^{+0.091+0.521+0.085}_{-0.289-0.187-0.046}$
$\bar{B}^0 \to K^0\bar{K}^0$	$-0.38^{+0.69}_{-0.77} \pm 0.09$ $-1.28^{+0.80+0.11}_{-0.73-0.16}$	(-0.110)	(0.184)	$0.327^{+0.264+0.072+0.002}_{-0.283-0.068-0.011}$
$\bar{B}^0 \to \pi^0\eta$	-	(0.019)	(0.064)	$0.057^{+0.151+0.011+0.000}_{-0.145-0.012-0.004}$
$\bar{B}^0 \to \pi^0\eta'$	-	(0.043)	(-0.011)	$0.084^{+0.064+0.016+0.0001}_{-0.124-0.018-0.003}$
$\bar{B}_s{}^0 \to \pi^+\pi^-$	-	(0.143)	(-0.003)	$0.095^{+0.055+0.109+0.002}_{-0.014-0.942-0.001}$
$\bar{B}_s{}^0 \to \pi^0\pi^0$	-	(0.143)	(-0.003)	$0.095^{+0.055+0.109+0.002}_{-0.014-0.942-0.001}$
$\bar{B}_s{}^0 \to \eta\eta$	-	(-0.041)	(-0.033)	$-0.057^{+0.029+0.016+0.003}_{-0.002-0.017-0.004}$
$\bar{B}_s{}^0 \to \eta\eta'$	-	(-0.006)	(-0.010)	$-0.016^{+0.016+0.005+0.001}_{-0.007-0.003-0.002}$
$\bar{B}_s{}^0 \to \eta'\eta'$	-	(0.031)	(0.033)	$0.048^{+0.013+0.003+0.000}_{-0.014-0.003-0.000}$
$\bar{B}_s{}^0 \to K^+K^-$	-	(0.194)	(0.202)	$0.195^{+0.019+0.017+0.005}_{-0.035-0.021-0.004}$
$\bar{B}_s{}^0 \to K^0\bar{K}^0$	-	(0.005)	(-0.007)	$-0.010^{+0.023+0.007+0.001}_{-0.010-0.005-0.002}$
$\bar{B}_s{}^0 \to \pi^0\eta$	-	(0.691)	(0.382)	$0.140^{+0.175+0.008+0.044}_{-0.230-0.007-0.025}$
$\bar{B}_s{}^0 \to \pi^0\eta'$	-	(0.816)	(0.597)	$0.135^{+0.169+0.095+0.065}_{-0.145-0.096-0.037}$
$\bar{B}_s{}^0 \to K_S\pi^0$	-	(-0.315)	(-0.719)	$-0.155^{+0.116+0.061+0.101}_{-0.147-0.047-0.164}$
$\bar{B}_s{}^0 \to K_S\eta$	-	(-0.137)	(-0.622)	$0.076^{+0.255+0.031+0.091}_{-0.416-0.050-0.157}$
$\bar{B}_s{}^0 \to K_S\eta'$	-	(-0.174)	(-0.256)	$0.001^{+0.046+0.077+0.001}_{-0.109-0.0848-0.001}$

of the state f. Comparing with the recent value of $\sin2\beta_{c\bar{c}K} = 0.671 \pm 0.024$ [2] as measured in $B^0 \to K +$ charmonium modes, we obtain

$$\Delta S(K_S\pi^0) = 0.107^{+0.028}_{-0.046}, \qquad \Delta S(K_S\eta) = 0.098^{+0.051}_{-0.068},$$
$$\Delta S(K_S\eta') = 0.011^{+0.026}_{-0.024}. \tag{30}$$

Note that the uncertainties in $\Delta S(K_S\eta')$ are dominated by the one in the $\sin2\beta_{c\bar{c}K}$ measurement. The $\Delta S(K_S\eta')$, being one of the promising tests of the SM [4], agrees with the one found in [4,5], while the $\Delta S(K_S\pi^0)$ given here is slightly larger. The main contribution to the $\chi^2_{\{S(\bar{B}^0)\}}$ given in Table I is from $S(\bar{B}^0 \to K^0\bar{K}^0)$.

We note that in the charming penguin approach by Ciuchini *et al.* [33], the $K\pi$ direct CP violation puzzle $\Delta\mathcal{A}(K\pi)$ can also be resolved [15] and predictions on ΔS are made. Ciuchini *et al.* obtained $\Delta S(K_S\pi^0) = 0.024 \pm 0.059$ and $\Delta S(K_S\eta') = -0.007 \pm 0.054$ [8,15]. Note that (i) their $\Delta S(K_S\pi^0)$ overlaps with the one given in this work, (ii) the central value of their $\Delta S(K_S\eta')$ is negative, but the associated uncertainties allow positive $\Delta S(K_S\eta')$ as well. There is a considerable overlap between their $\Delta S(K_S\eta')$ and the one given here.

For $\bar{B}^0_s$ decays, the S contributed from $\bar{B}^0_s$-B^0_s mixing itself is around -0.036. Hence, for penguin dominated $b \to s$ transition, such as $\bar{B}_s \to K^0\bar{K}^0$, $\eta^{(\prime)}\eta^{(\prime)}$ decays, we do not expect the corresponding $|S|$ to be much larger than $\mathcal{O}(0.05)$. Indeed, the predicted $|S|$ as shown in Table VI for $\bar{B}^0_s \to \eta\eta$, $\eta'\eta'$ and $\eta\eta'$ decays are all below 0.06. In particular, given the large $\bar{B}^0_s \to \eta^{(\prime)}\eta'$ rates, $S(\bar{B}_s \to \eta^{(\prime)}\eta')$ are potentially good places to test the standard model. Given the recent interesting preliminary results in the B_s phase [1,23], it will be very useful to search for S in these B_s charmless decays.

IV. CONCLUSION

In this work, we study the FSI effects in all charmless $\bar{B}_{u,d,s} \to PP$ decay modes. We consider a FSI approach with both short- and long-distance contributions in which the former are from all inelastic channels and are contained in factorization amplitudes, while the latter are from residual rescattering among PP states. Flavor SU(3) symmetry

is used to constrain the residual rescattering S matrix. We fit to all available data on the CP-averaged decay rates and CP asymmetries and make predictions on yet to be measured ones. Our main results are as follows:

(i) Results are in agreement with data in the presence of FSI.

(ii) The fitted strong phase $\phi_A \simeq -66^\circ$ in annihilation amplitudes is close to the one used in the S4 scenario of the QCDF approach.

(iii) For $\bar{B}$ decays, the $\pi^+\pi^-$ and $\pi^0\pi^0$ rates are suppressed and enhanced, respectively, by FSI.

(iv) The deviation ($\Delta\mathcal{A}$) between $\mathcal{A}(\bar{B}^0 \to K^-\pi^+)$ and $\mathcal{A}(B^- \to K^-\pi^0)$ can be understood in the FSI approach. Since $\mathcal{A}(K^-\pi^0)$ is more sensitive to the residual rescattering, the degeneracy of these two direct CP violations can be successfully lifted. However, both short- and long-distance strong phases are needed to give correct values for $\mathcal{A}(\bar{K}\pi)$s.

(v) It is interesting to note that the exchange rescattering is responsible for generating large and complex color-suppressed amplitudes, which are crucial in explaining the enhancements in the $\mathcal{B}(\bar{B}^0 \to \pi^0\pi^0)/\mathcal{B}(\bar{B}^0 \to \pi^+\pi^-)$ ratio and the CP asymmetry difference $\Delta\mathcal{A}$.

(vi) The residual FSI has a large impact on direct CP asymmetries of many modes.

(vii) The direct CP violation of $B^- \to \pi^-\pi^0$ is very small and does not receive any contribution from the residual rescattering [see Eq. (7)]. It remains as a clean mode to search for new physics phases.

(viii) The present data on $\bar{B}_s \to PP$ decay rates and direct CP violations can be successfully reproduced.

(ix) Several $\bar{B}_s$ decay rates are enhanced by FSI. In particular, the $\eta'\eta'$ branching ratio is predicted to reach 10^{-4} level, which can be checked experimentally.

(x) Time-dependent CP asymmetry S in $\bar{B}_{d,s}$ decays are studied. The $\Delta S(\bar{B}^0 \to K_S\eta')$ is very small ($\leq 1\%$). This asymmetry remains as one of the cleanest measurements to search for new physics phases. The fitted $\Delta S(\bar{B}^0 \to K_S\pi^0)$ is positive and cannot explain the present $\Delta S(\bar{B}^0 \to K_S\pi^0)$ data.

(xi) Most of the time-dependent CP asymmetries S of $\bar{B}_s$ to PP states with the strangeness $S = +1$ are expected to be small. The predicted $|S|$ for $\bar{B}_s^0 \to \eta\eta$, $\eta\eta'$ and $\eta'\eta'$ decays are all below 0.06. These modes will be useful to test the SM.

ACKNOWLEDGMENTS

The author is grateful to Paoti Chang, Hai-Yang Cheng, Hsiang-nan Li, and Amarjit Soni for helpful discussions. This work is supported in part by the National Science Council of R.O.C. under Grant Nos. NSC-95-2112-M-033-MY2 and NSC 97-2112-M-033-002-MY3.

APPENDIX A: MASTER FORMULA OF FSI

Let $H_W = \sum_q \lambda_q O_q$ denote the weak decay Hamiltonian, where λ_q are $V_{qb}V_{qd}^*$ (or $V_{qb}V_{qs}^*$) and O_q are four-quark operators (including Wilson coefficients c_is. From time reversal invariance of O_q, one has

$$\begin{aligned}\langle i;\text{out}|O_q|\bar{B}\rangle^* &= (\langle i;\text{out}|)^* U_T^\dagger U_T O_q^* U_T^\dagger U_T |\bar{B}\rangle^* \\ &= \langle i;\text{in}|O_q|\bar{B}\rangle \\ &= \sum_k \langle i;\text{in}|k;\text{out}\rangle\langle k;\text{out}|O_q|\bar{B}\rangle \\ &= \sum_k \mathcal{S}_{ki}^*\langle k;\text{out}|O_q|\bar{B}\rangle, \end{aligned} \tag{A1}$$

where $\mathcal{S}_{ik} \equiv \langle i;\text{out}|k;\text{in}\rangle$ is the strong interaction S-matrix element, and we have used $U_T|\text{out(in)}\rangle^* = |\text{in(out)}\rangle$ to fix the phase convention. Equation (A1) can be solved by (see, for example [48])

$$\langle i;\text{out}|O_q|\bar{B}\rangle = \sum_k \mathcal{S}_{ik}^{1/2} A_k^{q0}, \tag{A2}$$

where A_k^{q0} is a real amplitude. To show that this is indeed a solution to Eq. (A1), one needs to use $\mathcal{S}_{ik} = \mathcal{S}_{ki}$, which follows from the time reversal invariance of strong interactions and the phase convention we have adopted. The weak decay amplitude picks up strong scattering phases [49], and we have

$$\begin{aligned} A_i^{\text{FSI}} &= \langle i;\text{out}|H_W|\bar{B}\rangle = \sum_q \langle i;\text{out}|\lambda_q O_q|\bar{B}\rangle \\ &= \sum_{q,k} \mathcal{S}_{ik}^{1/2}(\lambda_q A_k^{q0}) = \sum_k \mathcal{S}_{ik}^{1/2} A_k^0, \end{aligned} \tag{A3}$$

where we have defined $A^0 \equiv \sum_q \lambda_q A^{q0}$ free of any strong phase. The above equation is the master formula for FSI in $\bar{B}_{u,d,s}$ decays.

APPENDIX B: CONSTRAINTS IN THE U(3) CASE

In the U(3) case, one cannot have rescattering from both exchange and annihilation so that $r_e^{(m)} r_a^{(m)} = 0$. This can be easily seen by inspecting $\mathcal{S}_{\text{res},3}^m$ in the $\pi^-\pi^0 - K^0K^- - \pi^-\eta_q - \pi^-\eta_s$ basis, where $\eta_q = (u\bar{u} + d\bar{d})/\sqrt{2}$ and $\eta_s = s\bar{s}$. From Eq. (9) and the requirement that $\mathcal{S}_{\text{res}}^m$ and $\mathcal{T}^{(m)}$ preserve their forms as determined by U(3) symmetry, we should have

$$\mathcal{T}^{(m)} = \begin{pmatrix} r_0^{(m)} + r_a^{(m)} & 0 & 0 & 0 \\ 0 & r_0^{(m)} + r_a^{(m)} & \sqrt{2} r_a^{(m)} & r_e^{(m)} \\ 0 & \sqrt{2} r_a^{(m)} & r_0^{(m)} + 2r_a + r_e^{(m)} & 0 \\ 0 & r_e^{(m)} & 0 & r_0^{(m)} \end{pmatrix} \tag{B1}$$

in the new basis. Under U(3) symmetry, it is evident that $(\mathcal{S}^m_{\mathrm{res},3})_{34,43} = 0$ for any m. Hence, from

$$(\mathcal{S}^{2m}_{\mathrm{res},3})_{34,43} = (1 + 2i\mathcal{T}^{(m)}_3 - \mathcal{T}^{(m)}_3 \cdot \mathcal{T}^{(m)}_3)_{34,43} = -\sqrt{2} r^{(m)}_e r^{(m)}_a, \tag{B2}$$

which should also be zero, we must have

$$r^{(m)}_e r^{(m)}_a = 0 \tag{B3}$$

for any m in the U(3) case.

Given the above constraint, we have two different solutions, which are, (a) annihilation-type ($r^{(m)}_a \neq 0$, $r^{(m)}_e = 0$) and (b) exchange-type ($r^{(m)}_e \neq 0$, $r^{(m)}_a = 0$). For the annihilation-type solution, we have

$$\begin{aligned} 1 + i(r^{(m)}_0 + r^{(m)}_a) &= \frac{2e^{2mi\bar{\delta}} + 3e^{2mi\delta_8}}{5}, \\ ir^{(m)}_a &= \frac{3}{5}(e^{2mi\delta_8} - e^{2mi\bar{\delta}}), \\ i(r^{(m)}_a + r^{(m)}_t) &= \frac{-e^{2mi\bar{\delta}} - 4e^{2mi\delta_8} + 5e^{2mi\delta_1}}{20}, \\ r^{(m)}_e &= 0, \end{aligned} \tag{B4}$$

which corresponds to taking

$$\delta_{27} = \delta'_8 = \delta'_1 \equiv \bar{\delta}, \qquad \delta_8, \delta_1, \tau = -\frac{1}{2}\sin^{-1}\frac{4\sqrt{5}}{9}, \qquad \nu = -\frac{1}{2}\sin^{-1}\frac{4\sqrt{2}}{9} \tag{B5}$$

in Eq. (15). For the exchange-type solution, we have

$$\begin{aligned} 1 + ir^{(m)}_0 &= \frac{1}{2}(e^{2mi\bar{\delta}} + e^{2mi\delta_8}), \\ ir^{(m)}_e &= \frac{1}{2}(e^{2mi\bar{\delta}} - e^{2mi\delta_8}), \qquad r^{(m)}_a = r^{(m)}_t = 0, \end{aligned} \tag{B6}$$

which corresponds to setting

$$\delta_{27} = \delta'_8 = \delta'_1 \equiv \bar{\delta}, \qquad \delta_8 = \delta_1, \qquad \tau = \frac{1}{2}\sin^{-1}\frac{\sqrt{5}}{3}, \qquad \nu = \frac{1}{2}\sin^{-1}\frac{2\sqrt{2}}{3} \tag{B7}$$

in Eq. (15).

In the above solutions, we explicitly see that U(3) symmetry imposes relations on the parameters of different SU(3) multiplets, and, consequently, reduces the number of independent parameters. It should be noted that mixing angles are fixed in both solutions.

[1] C. Amsler *et al.* (Particle Data Group), Phys. Lett. B **667**, 1 (2008).

[2] E. Barberio *et al.* (Heavy Flavor Averaging Group (HFAG)), arXiv:0808.1297; online update at http://www.slac.stanford.edu/xorg/hfag.

[3] Y. Grossman and M. P. Worah, Phys. Lett. B **395**, 241 (1997); D. London and A. Soni, Phys. Lett. B **407**, 61 (1997); Y. Grossman, G. Isidori, and M. P. Worah, Phys. Rev. D **58**, 057504 (1998); Y. Grossman, Z. Ligeti, Y. Nir, and H. Quinn, Phys. Rev. D **68**, 015004 (2003); M. Gronau, Y. Grossman, and J. L. Rosner, Phys. Lett. B **579**, 331 (2004); M. Gronau, J. L. Rosner, and J. Zupan, Phys. Lett. B **596**, 107 (2004).

[4] H. Y. Cheng, C. K. Chua, and A. Soni, Phys. Rev. D **72**, 014006 (2005).

[5] M. Beneke, Phys. Lett. B **620**, 143 (2005).

[6] See also, C. K. Chua, in *Proceedings of 4th Flavor Physics and CP Violation Conference (FPCP 2006), Vancouver, British Columbia, Canada, 2006*, edited by C. Hearty, eConf C060409, 008 (2006); arXiv:0807.3596.

[7] M. Gronau, J. L. Rosner, and J. Zupan, Phys. Rev. D **74**, 093003 (2006).

[8] M. Artuso *et al.*, arXiv:0801.1833.

[9] Y. Y. Keum, H. n. Li, and A. I. Sanda, Phys. Lett. B **504**, 6 (2001); Phys. Rev. D **63**, 054008 (2001).

[10] M. Beneke, G. Buchalla, M. Neubert, and C. T. Sachrajda, Nucl. Phys. **B606**, 245 (2001).

[11] A. J. Buras, R. Fleischer, S. Recksiegel, and F. Schwab, Nucl. Phys. **B697**, 133 (2004).

[12] A. J. Buras, R. Fleischer, S. Recksiegel, and F. Schwab, Acta Phys. Pol. B **36**, 2015 (2005).

[13] A. J. Buras, R. Fleischer, S. Recksiegel, and F. Schwab, Eur. Phys. J. C **45**, 701 (2006).

[14] H. n. Li, S. Mishima, and A. I. Sanda, Phys. Rev. D **72**, 114005 (2005).

[15] M. Pierini, J. Phys. Conf. Ser. **110**, 052045, (2008); M. Ciuchini *et al.* (unpublished).

[16] S. Baek, P. Hamel, D. London, A. Datta, and D. A. Suprun, Phys. Rev. D **71**, 057502 (2005); S. Baek, J. High Energy Phys. 07 (2006) 025; S. Baek and D. London, Phys. Lett. B **653**, 249 (2007).

[17] W. S. Hou, H. n. Li, S. Mishima, and M. Nagashima, Phys. Rev. Lett. **98**, 131801 (2007).

[18] C. S. Kim, S. Oh, and Y. W. Yoon, Phys. Lett. B **665**, 231 (2008).

[19] S.-W. Lin *et al.* (Belle Collaboration), Nature (London) **452**, 332 (2008).

[20] W. S. Hou and K. C. Yang, Phys. Rev. Lett. **84**, 4806 (2000); **90**, 039901(E) (2003).

[21] C. K. Chua, W. S. Hou, and K. C. Yang, Phys. Rev. D **65**, 096007 (2002); C. K. Chua and W. S. Hou, Phys. Rev. D **72**, 036002 (2005); **77**, 116001 (2008).

[22] H. Y. Cheng, C. K. Chua, and A. Soni, Phys. Rev. D **71**, 014030 (2005).

[23] M. Bona *et al.* (UTfit Collaboration), arXiv:0803.0659; Diego Tonelli, in ICHEP 2008, Philadelphia, 2008, edited by A. J. S. Smith *et al.* (to be published); John Ellison, in ICHEP 2008, Philadelphia, 2008, edited by A. J. S. Smith *et al.* (to be published).
[24] M. Beneke and M. Neubert, Nucl. Phys. **B675**, 333 (2003); **B651**, 225 (2003).
[25] C. W. Bauer, S. Fleming, D. Pirjol, and I. W. Stewart, Phys. Rev. D **63**, 114020 (2001); C. W. Bauer, D. Pirjol, I. Z. Rothstein, and I. W. Stewart, Phys. Rev. D **70**, 054015 (2004).
[26] W. S. Hou (private communication).
[27] C. K. Chua, W. S. Hou, and K. C. Yang, Mod. Phys. Lett. A **18**, 1763 (2003).
[28] C. Smith, Eur. Phys. J. C **10**, 639 (1999); **33**, 523 (2004).
[29] J. F. Donoghue, E. Golowich, A. A. Petrov, and J. M. Soares, Phys. Rev. Lett. **77**, 2178 (1996).
[30] P. Zenczykowski and P. Lach, Phys. Rev. D **69**, 094021 (2004).
[31] M. Suzuki, Phys. Rev. D **77**, 054021 (2008).
[32] Y. L. Wu, Y. F. Zhou, and C. Zhuang, arXiv:0712.2889.
[33] M. Ciuchini, E. Franco, G. Martinelli, and L. Silvestrini, Nucl. Phys. **B501**, 271 (1997); A. J. Buras and L. Silvestrini, Nucl. Phys. **B569**, 3 (2000).
[34] T. Feldmann, P. Kroll, and B. Stech, Phys. Rev. D **58**, 114006 (1998); Phys. Lett. B **449**, 339 (1999).
[35] T. D. Lee, Contemp. Concepts Phys. **1**, 1 (1981).
[36] T. N. Pham, Phys. Rev. D **77**, 014024 (2008); **77**, 019905 (E) (2008).
[37] B. Aubert *et al.* (BABAR Collaboration), Phys. Rev. D **78**, 011107 (2008); W. Ford, FPCP 2008, Taipei, 2008, edited by P. Chang and H-n. Li (to be published in eConf); B. Aubert *et al.* (BABAR Collaboration), arXiv:0807.4226.
[38] A. Warburton, 6th Flavor Physics and *CP* Violation Conference (FPCP 2008), Taipei, 2008, edited by P. Chang and H-n. Li (to be published in eConf).
[39] J. Charles *et al.* (CKMfitter Group), Eur. Phys. J. C **41**, 1 (2005); online update at http://ckmfitter.in2p3.fr/.
[40] H. Y. Cheng, C. K. Chua, and C. W. Hwang, Phys. Rev. D **69**, 074025 (2004).
[41] D. Melikhov and B. Stech, Phys. Rev. D **62**, 014006 (2000).
[42] P. Ball, V. M. Braun, and A. Lenz, J. High Energy Phys. 05 (2006) 004; G. Duplancic, A. Khodjamirian, T. Mannel, B. Melic, and N. Offen, J. High Energy Phys. 04 (2008) 014.
[43] C. W. Chiang, M. Gronau, J. L. Rosner, and D. A. Suprun, Phys. Rev. D **70**, 034020 (2004); Y. Y. Charng and H. n. Li, Phys. Rev. D **71**, 014036 (2005).
[44] H. Ishino *et al.* (Belle Collaboration), Phys. Rev. Lett. **98**, 211801 (2007).
[45] J. M. Gerard and W. S. Hou, Phys. Rev. Lett. **62**, 855 (1989); D. Atwood, S. Bar-Shalom, G. Eilam, and A. Soni, Phys. Rep. **347**, 1 (2001).
[46] B. Aubert *et al.* (BABAR Collaboration), Phys. Rev. Lett. **97**, 171805 (2006).
[47] K. Abe *et al.* (Belle Collaboration), arXiv:0708.1845.
[48] M. Suzuki and L. Wolfenstein, Phys. Rev. D **60**, 074019 (1999).
[49] K. M. Watson, Phys. Rev. **88**, 1163 (1952).